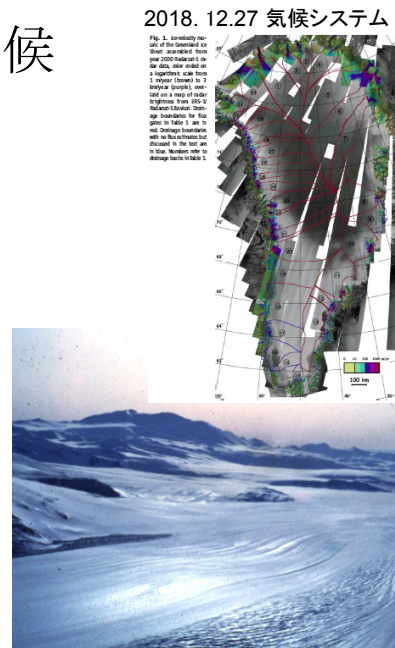


氷床と海水準と気候

東京大学大気海洋研究所
阿部彩子

Ref.
IPCC AR5 (第5次報告書, WG1, 2013)
Golledge et al, 2015, Nature
DeConte and Pollard, 2016, Nature
IMBIE team, 2018, Nature
Fyke et al, 2018, Rev. of Geophysics
Pattyn et al, 2018, Nature Clim. Change
Obase, Abe-Ouchi, Kusahara, Hasumi 2017, J. Clim.
Abe-Ouchi, et al, 2013, Nature



ポイント

- IPCCAR5までは、経験則が多く、また南極の不安定性が物理的に扱われなかつた。(経験則による予測は不自然なほど大きかつた)。
- その後の研究で、予測が海水準にして20cmほど加わり、21C末の予測がRCP8.5では1mを超えた。
- 南極の力学的寄与が不確実
- 海洋が氷床棚氷部分をどれほど融かし、それが内部からの氷床の流動や流出にどれほど寄与するか?大気が氷床表面を融かした結果がどれほど氷床崩壊に結びつくか?このような現象について、推定幅が広い。
- 気候と氷床について過去の氷床が大きく変化した時代状況をモデリングすることが課題となる

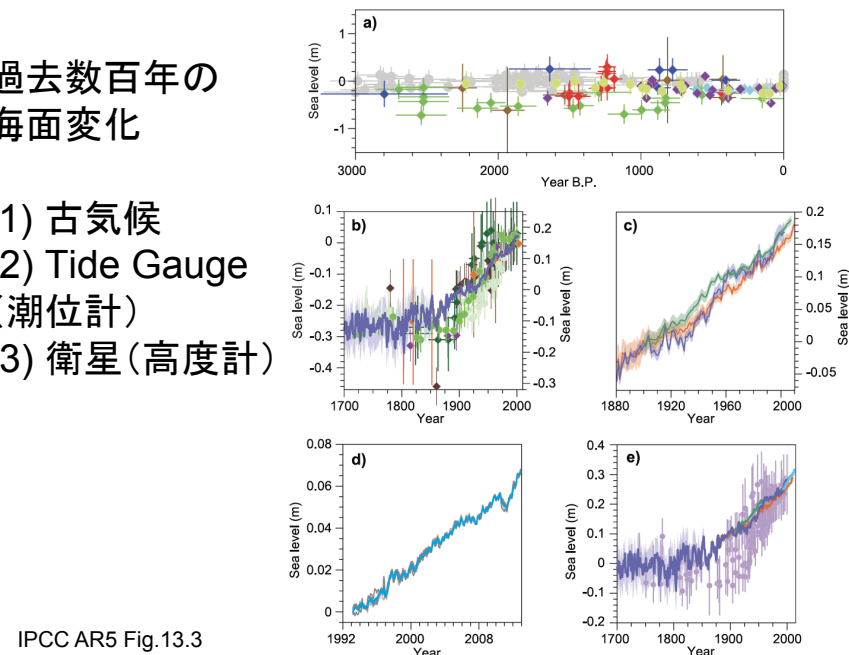
Contents

1. Observation of Ice sheet and Sea Level Change 氷床と海水準変化の観測
2. Cause of Sea level change and its estimation for the 20 century 海水準変化の原因
3. Global climate projection 将来予測の方法
4. Modelling the past and future ice sheet change 過去の変化の再現と将来予測
5. Summary まとめ

Global Sea Level Rise = Ocean Volume / Global Ocean area
海水準変化の定義：海水の体積変化／全海洋面積

過去数百年の海面変化

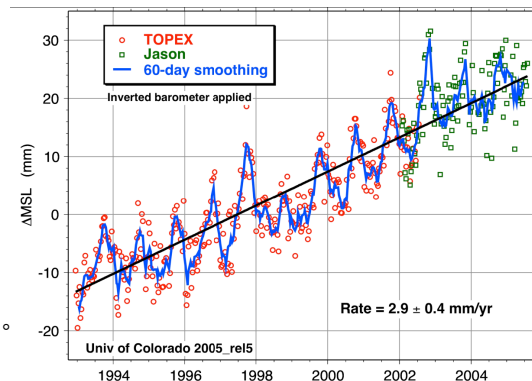
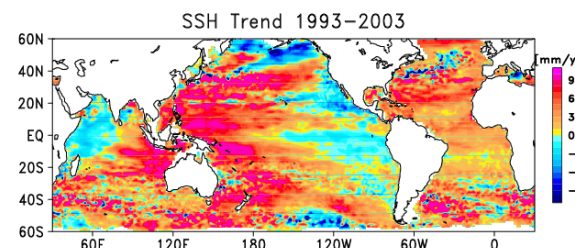
- (1) 古気候
- (2) Tide Gauge (潮位計)
- (3) 衛星(高度計)



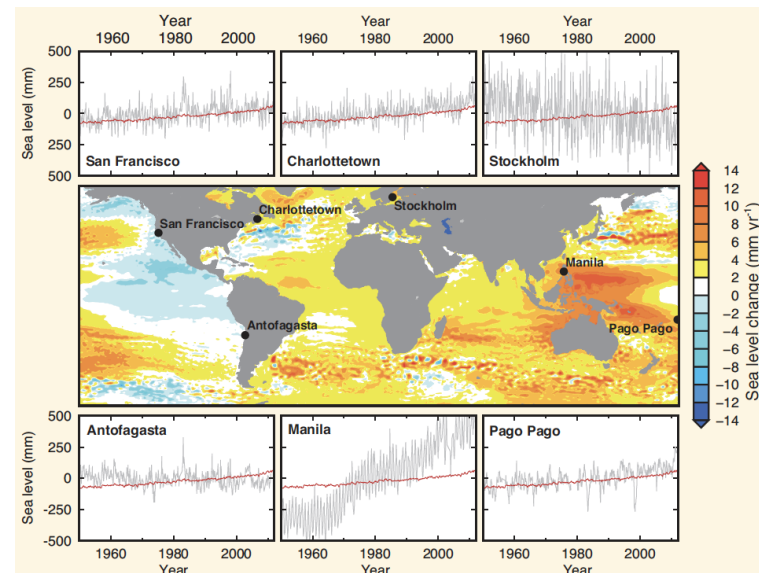
IPCC AR5 Fig.13.3

衛星データによる海 水準推定 Observed Sea level change by satellite

Continuous Increase of Sea level,
Although a regional difference!
平均した海面上昇が観測されている。
~ 3 mm in 1 year



最近の各地の海面変化



海水準変化の原因 Cause of Sea level change

短期的には、潮の満ち引き、嵐、エルニーニョや太平洋十年規模変動などの気候変動による。(風向風速、海流、温度、塩分などの変化が地域的な海面に変化を与える。)

長期的に(数年以上)は、

1. 海水の熱膨張 Thermal Expansion of ocean water
2. 南極やグリーンランド氷床の質量変化 Mass change of Antarctica and Greenland ice sheet
3. 山岳氷河の質量変化 (Mass change of Mountain Glaciers)
4. 固体地球の変形による長期変化、テクトニクス変動や後氷期による地球変形 (Long term change due to tectonics and post-glacial rebound)

海面上昇に関わるプロセス

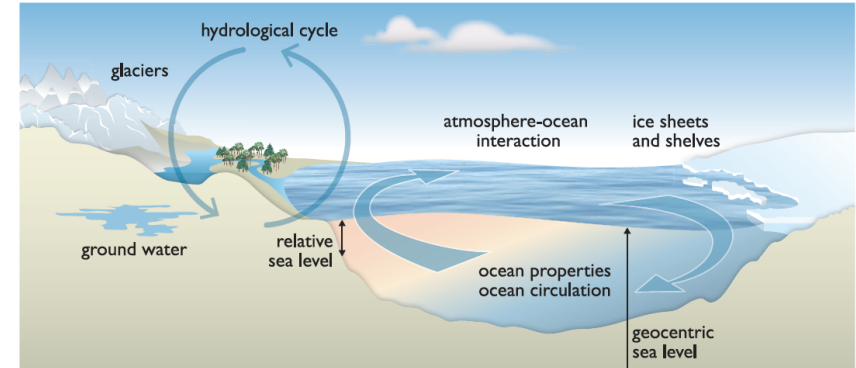
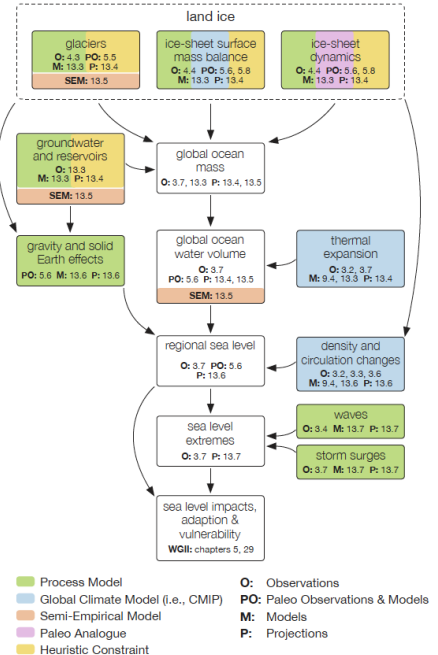
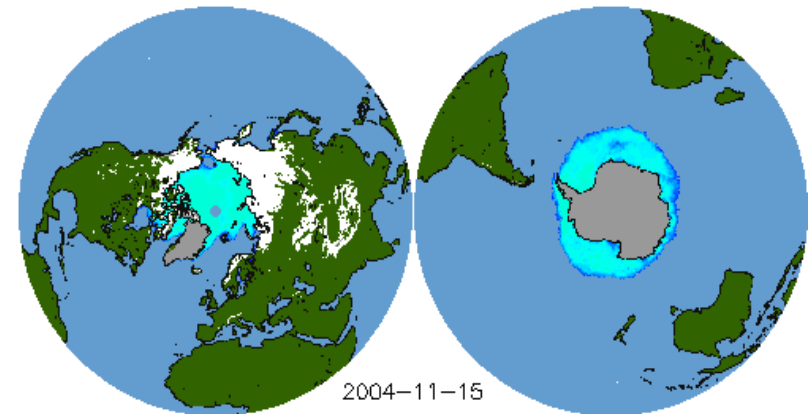


Figure 13.1 | Climate-sensitive processes and components that can influence global and regional sea level and are considered in this chapter. Changes in any one of the components or processes shown will result in a sea level change. The term 'ocean properties' refers to ocean temperature, salinity and density, which influence and are dependent on ocean circulation. Both relative and geocentric sea level vary with position. Note that the geocenter is not shown.



世界の雪と氷

雪(白)と氷河(灰色)と海氷(水色)



山岳氷河



Rhone Glacier
In Switzerland
スイスのローヌ氷河



現在気候下で存在する2つの大陸氷床

グリーンランド氷床



面積 : $1.80 \times 10^6 \text{ km}^2$ (陸地の1.2%)
体積 : $2.85 \times 10^6 \text{ km}^3$
海水準相当 : 7.36 m

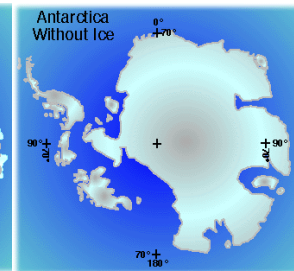
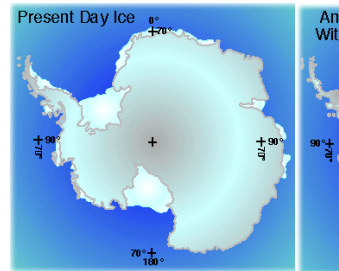
南極氷床が全て融解すると...
駒場 (34 m)、本郷 (20 m)、柏 (20 m) キャンパスは全て水没 (国土地理院)

南極氷床

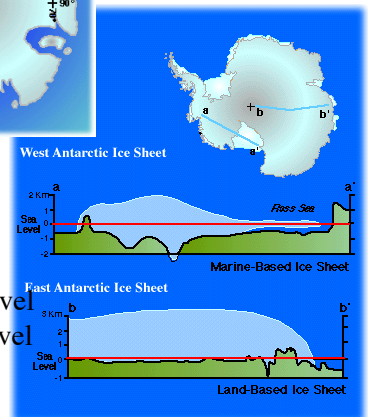


面積 : $12.30 \times 10^6 \text{ km}^2$ (陸地の8.3%)
体積 : $26.5 \times 10^6 \text{ km}^3$
海水準相当 : 58.3 m

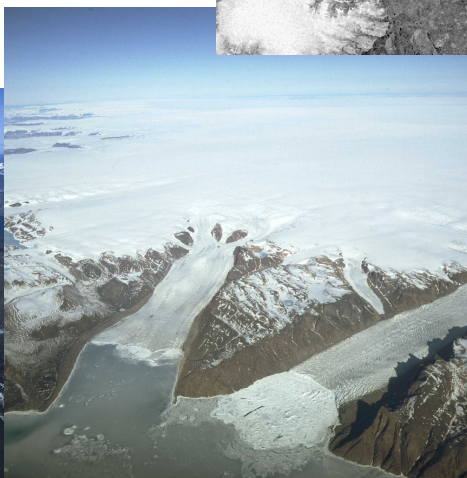
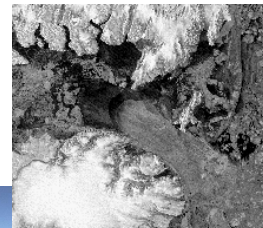
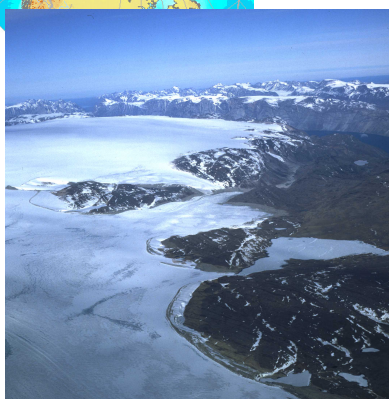
南極氷床 大陸規模氷河



90% の淡水は氷床にある。
南極、グリーンランドの氷床が融ければ、各々
70m, 7m 海面上昇する



グリーンランド氷床



内陸と沿岸域の雪氷表面の違い



氷床は陸起源

氷床と海水は異なるもの!!!

海水(sea ice)：
海水が凍結して
海に浮いているもの、
厚さ～1m



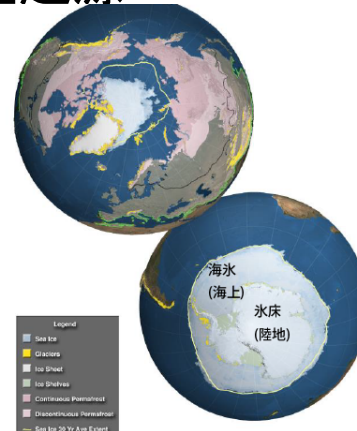
氷床,棚氷(ice shelf)
：陸上に降った雪が
固まったもの、
厚さ～数百m
海洋でてくると
氷山(iceberg)とよばれる



https://nsidc.org/sites/nsidc.org/files/images/seaside_04.jpg
<https://www.nasa.gov/image-feature/getting-to-know-the-ice-shelf>

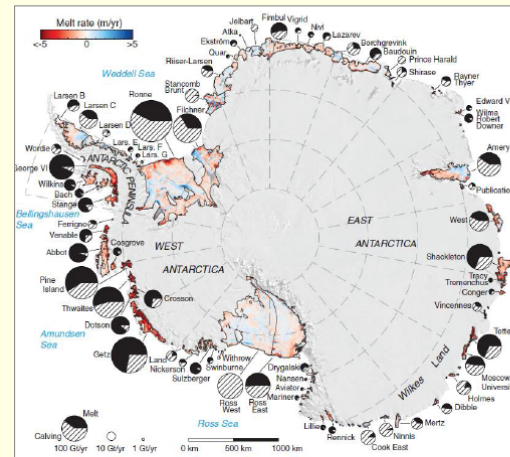
- ・氷床のうち、海に張り出しているものを棚氷(ice shelf)とよぶ
- ・南極の海岸線のおよそ半分、面積のおよそ1割が棚氷

海水は海面上昇に寄与しないが、大気や海洋や氷床との相互作用を通じて気候や海面変化における役割は重要)



IPCC AR5 Fig. 4.1

南極氷床の質量収支



棚氷底面融解量・氷山分離量の分布 (Gt/yr) Rignot et al. 2013

| | 質量収支(Gt/yr) |
|--------|-------------|
| 涵養量 | 2240～2295 |
| 棚氷底面融解 | -1325±235 |
| 氷山分離 | -1089±139 |

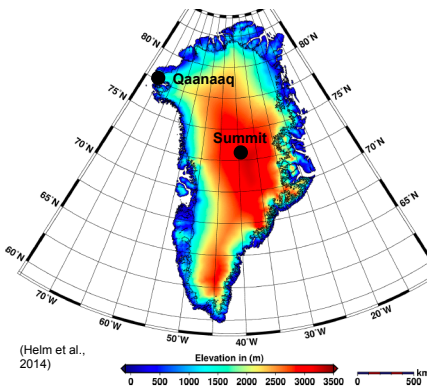
涵養量 : Wild et al. 2003; Crinner et al. 2006
棚氷底面融解, 氷山分離 : Rignot et al. 2013

大気による氷床の融解は小さい

海洋からの熱による融解・氷山の分離が主要な消耗プロセス

氷床の地形 | 内陸と沿岸域の気温

グリーンランド氷床

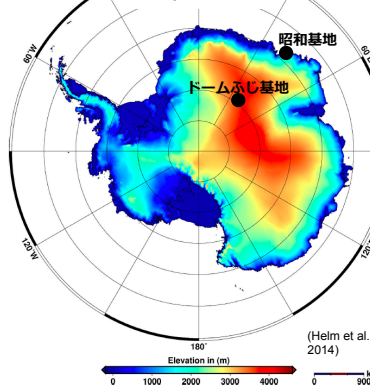


年平均気温

沿岸 : -8°C (Qaanaaq; 16 m)
内陸 : -29°C (Summit; 3208 m)

(Sugiyama et al., 2014; Steffen and Box, 2001)

南極氷床



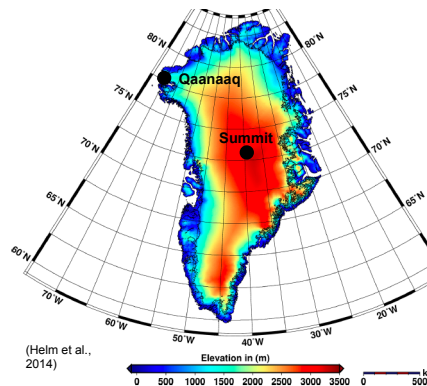
年平均気温

沿岸 : -10°C (昭和基地; 29 m)
内陸 : -54°C (DF基地; 3810m)

(気象庁, 国立極地研究所)

氷床の地形 | 内陸と沿岸域の気温

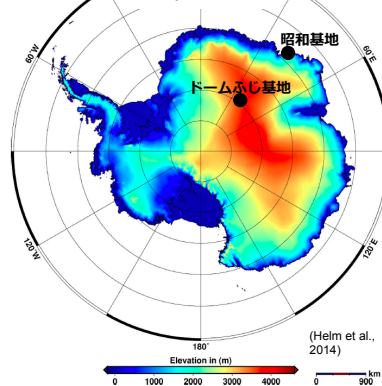
グリーンランド氷床



年平均気温

沿岸 : -8°C (Qaanaaq; 16 m)
内陸 : -29°C (Summit; 3208 m)

南極氷床



年平均気温

沿岸 : -10°C (昭和基地; 29 m)
内陸 : -54°C (DF基地; 3810m)

(気象庁, 国立極地研究所)

南極とグリーンランド氷床の降水量

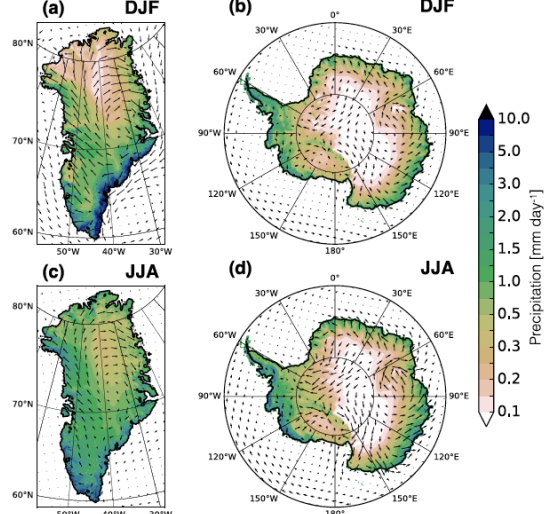
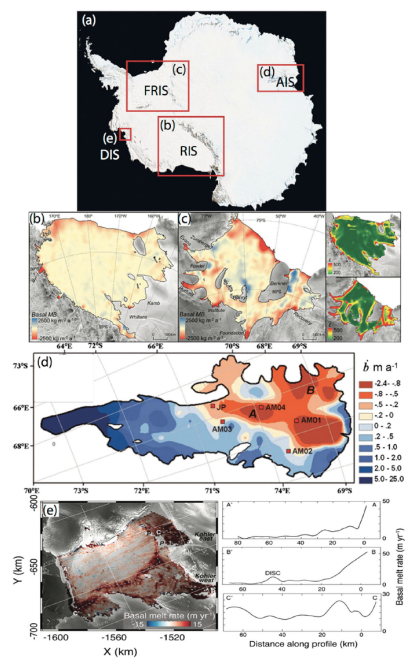


Figure 4. Daily average precipitation (mm/day) (shading) and 10 m wind (arrows) in (a, b) the December, January, and February (DJF) and (c, d) June, July, and August (JJA) seasons, separated between (a, c) Greenland and (b, d) Antarctica. The longest arrows correspond to approximately 10 m/s. Data are adopted from the Regional Atmospheric Climate Model version 2.3 (van den Broeke et al., 2017; van Wessem et al., 2018).

南極の棚氷における融解分布



グリーンランド氷床の表面融解

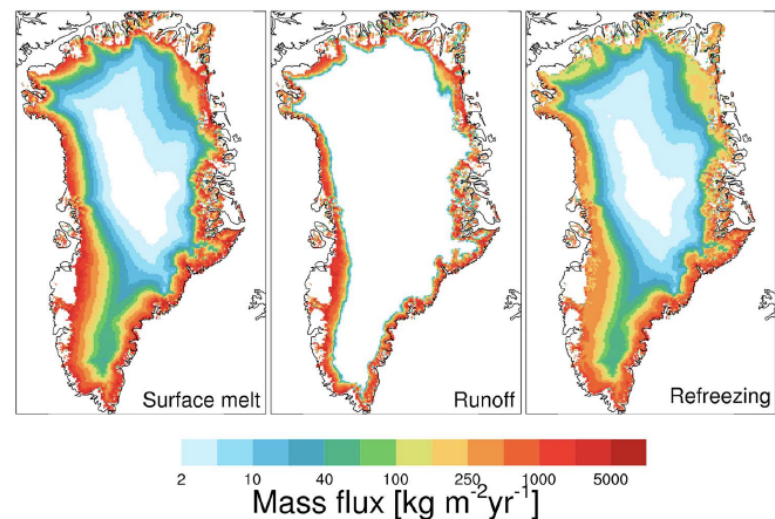


Figure 6. GrIS surface melt and resulting runoff versus refreezing as simulated by Regional Atmospheric Climate Model version 2 (Noël et al., 2017).

南極氷床の平均流動速度(2007-2009年)



Rignot et al. (2011) Science
<http://svs.gsfc.nasa.gov/3849>

南極とグリーンランドにおける氷床 流動速度分布

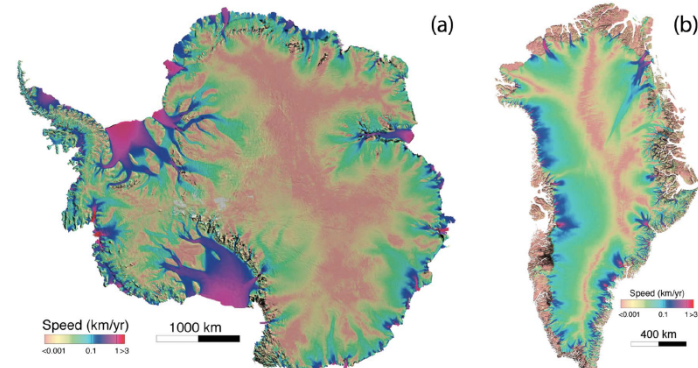


Figure 9. (a) Antarctic ice sheet surface velocity. (b) Greenland ice sheet surface velocity. Figures are reproduced with permission from Mouginot et al. (2017).

氷床の融解による地形や海面の変化

B 粘弾性地球の応答

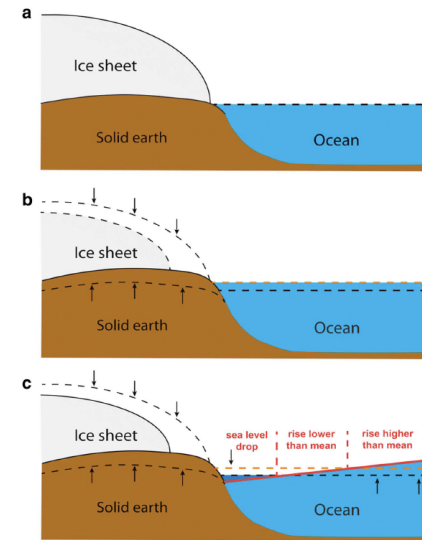
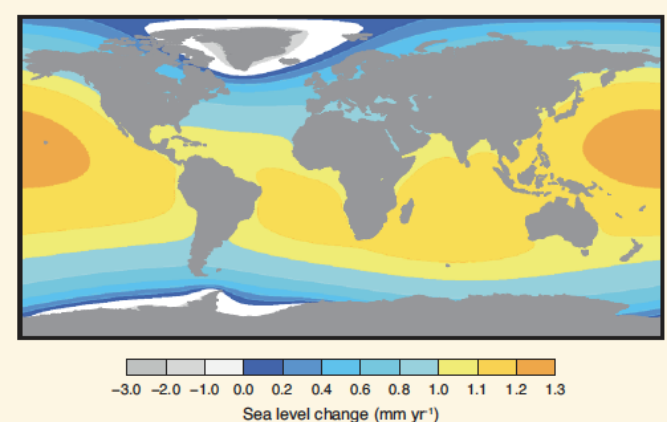


Figure 13. Schematic illustration showing the impacts of ice sheet, viscoelastic, and gravitational model coupling on simulated sea level change. (a) An initial, equilibrium ice sheet (gray), solid Earth (brown), and ocean (blue) configuration. (b) Only the ice sheet and viscoelastic Earth models are coupled, so that a reduction in ice thickness (e.g., via a mass balance perturbation) leads to uplift of the bedrock beneath the ice sheet and a uniform increase in sea level (dashed black lines indicate initial reference surfaces). (c) When a gravitation model is also coupled, simulated ice sheet mass loss also leads to a simulated sea level drop proximal to the ice sheet and SLR far from the ice sheet (solid red line), relative to the case with no gravitational coupling (dashed red line). The image has been reproduced with permission from de Boer et al. (2017).

氷床融解と地球変形による海面上昇も



FAQ13.1, Figure 2 | Model output showing relative sea level change due to melting of the Greenland ice sheet and the West Antarctic ice sheet at rates of 0.5 mm yr^{-1} each (giving a global mean value for sea level rise of 1 mm yr^{-1}). The modelled sea level changes are less than the global mean value in areas

氷床の外力に対する応答

Fyke, et al, 2017, Rev. Geo

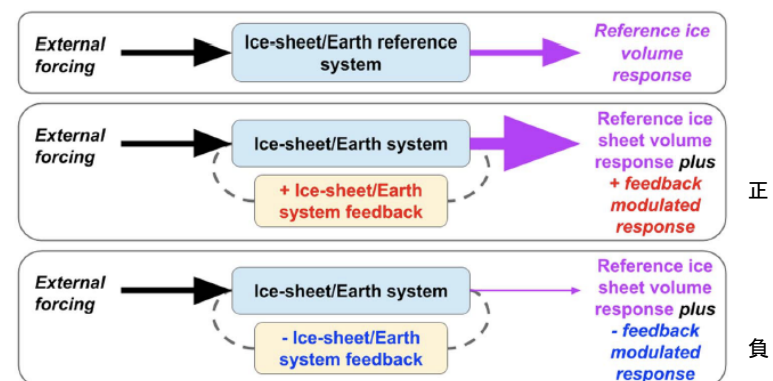
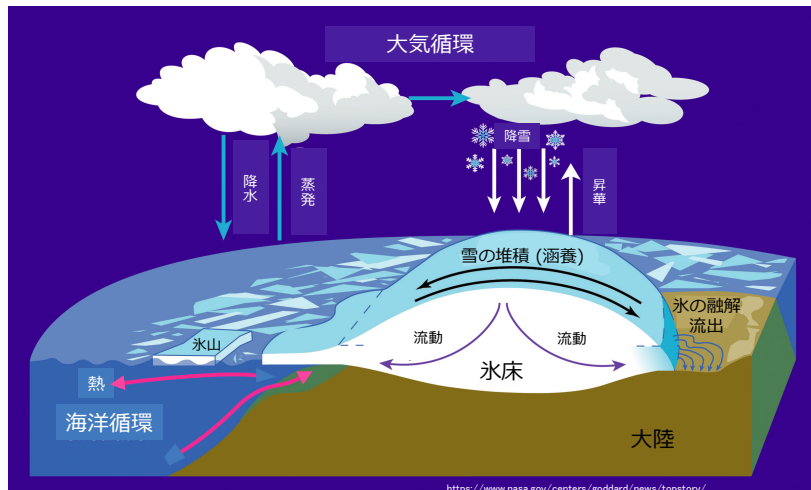


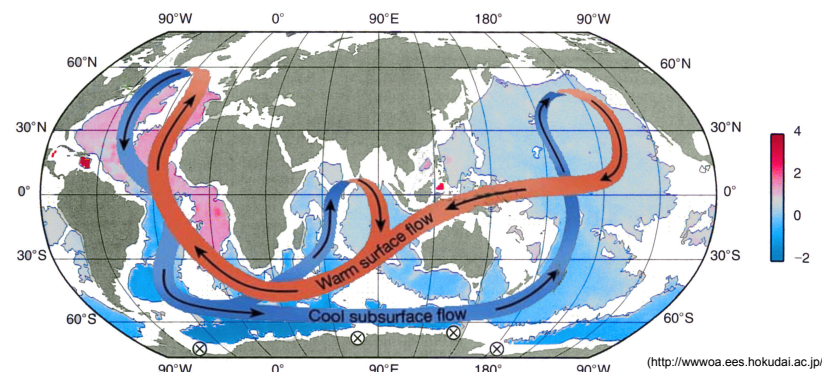
Figure 10. Schematic illustrating the operation of ice sheet/Earth system feedbacks. External forcings (forcings that are

地球システムにおける気候－海洋－氷床



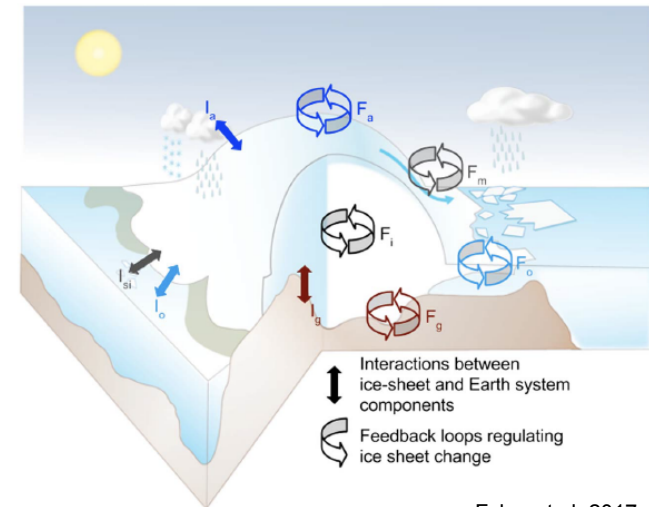
氷床の変動は、大気・海洋の変動と密接に関係している

熱塩循環：氷床と密接な関係



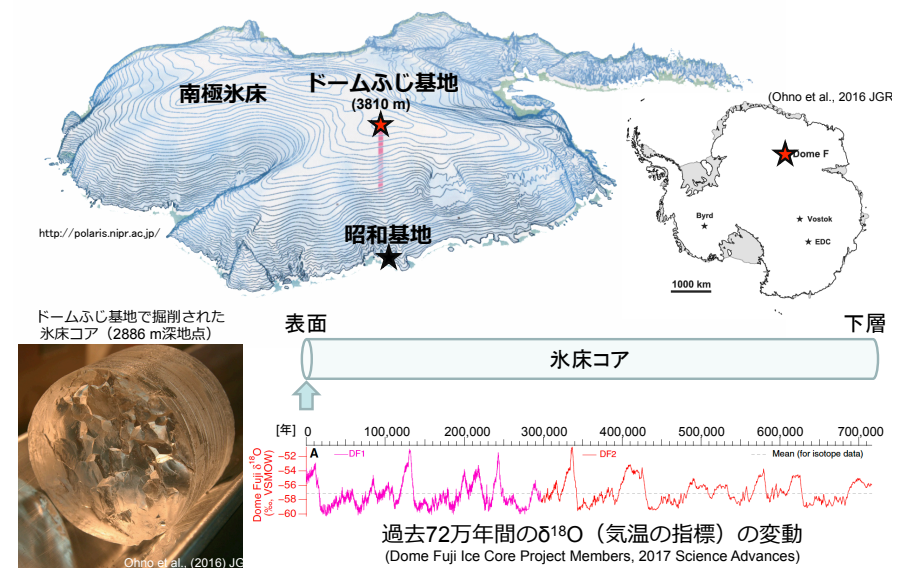
おもに中深層（数百メートル以深）で起こる地球規模の海洋循環海水の「温度」と「塩分濃度」の変化で駆動される

表層 → 深層：北大西洋
深層 → 表層：インド洋、北太平洋

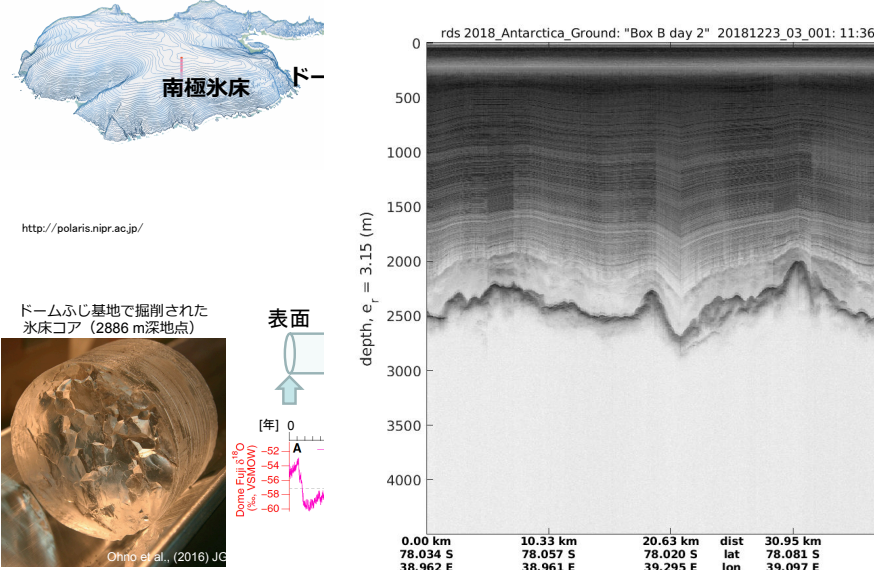


Fyke, et al., 2017, Rev. Geo

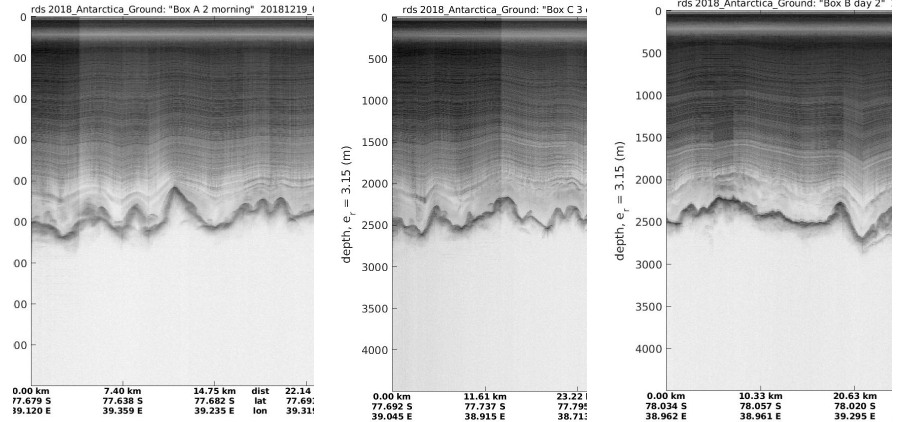
南極ドームふじ基地で掘削された氷床コア



南極New Dome Fuji 基地周辺の氷床内部（レーダー）



南極New Dome Fuji 基地周辺の氷床内部（レーダー）



氷床モデル

氷床力学を記述する方程式系

基本的には流体力学 (非ニュートン性流体 → 応力とひずみ速度の関係が非線形)

主要な式：

運動方程式

$$\rho \frac{\partial \mathbf{v}}{\partial t} = \nabla \cdot \boldsymbol{\sigma} + \rho \mathbf{g}$$

加速度項 応力(stress) 重力
 テンソル

式が意味すること：

→重力と応力がつりあう

質量保存の式

$$\frac{\partial H}{\partial t} = -\nabla \cdot (\bar{\mathbf{v}}H) + m_s - m_b$$

氷厚さ 氷の 滲養量 融解量
 時間変化 (流入・流出) (流出・流入)

→氷の厚さ変化は氷の
 流入、流出と滲養・融解の和

構成方程式

$$\dot{\epsilon} = mA(T) \tau_e'^{n-1} \sigma'$$

ひずみ速度 応力第二 deviatoric
 不变量 stress m, A(T): 応力に対する
 变形のしやすさを表すパラメータ

→氷の変形が流動に現れる

→温度は移流と拡散で決まる

大気海洋との違い：流れが診断的（流れの時間微分が流れに直接よらない）
 →基本的には時間・空間スケールの問題

氷床モデリング

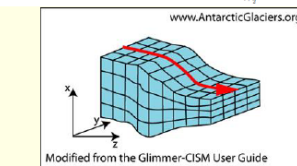
モデルを作ってうごかしてみる：近似、離散化、プログラムの作成

- 氷床の空間スケール近似
 (静水圧, Shallow Ice Approximation)

$$\begin{aligned} \frac{\partial \sigma_{xx}}{\partial x} + \frac{\partial \sigma_{xy}}{\partial y} + \frac{\partial \sigma_{xz}}{\partial z} &= 0 \\ \frac{\partial \sigma_{xy}}{\partial x} + \frac{\partial \sigma_{yy}}{\partial y} + \frac{\partial \sigma_{yz}}{\partial z} &= 0 \\ \frac{\partial \sigma_{xz}}{\partial x} + \frac{\partial \sigma_{yz}}{\partial y} + \frac{\partial \sigma_{zz}}{\partial z} &= \rho g \\ \sigma_{xx} = \sigma_{yy} = \sigma_{zz} &= -p \end{aligned}$$

- 数値計算のための離散化
 例として質量保存の式：

$$\begin{aligned} \frac{\partial H}{\partial t} &= -\frac{1}{dx} (D_{i+\frac{1}{2}} \frac{H_{i+1} - H_i}{dx_{i+\frac{1}{2}}} - D_{i-\frac{1}{2}} \frac{H_i - H_{i-1}}{dx_{i-\frac{1}{2}}}) - \frac{1}{dx} (a_{Bi+\frac{1}{2}} \frac{H_{i+1} + H_i}{2} - a_{Bi-\frac{1}{2}} \frac{H_i + H_{i-1}}{2}) \\ &\quad - \frac{1}{dx} (D_{i+\frac{1}{2}} \frac{b_{i+1} - b_i}{dx_{i+\frac{1}{2}}} - D_{i-\frac{1}{2}} \frac{b_i - b_{i-1}}{dx_{i-\frac{1}{2}}}) + a_s + a_b \end{aligned}$$



- X-Z平面で計算するルーチンの作成

[0] 時刻=0

- すべてのnx[xグリッド数]に対して
 - 氷厚Hからs, ∇s , ∇H を求める
 - 運動方程式からuの鉛直分布を求める
 - uの鉛直平均値から(uH)を求める
 - 氷厚Hの時間発展を記述する
 nx個の連立方程式を立てる
 - [2] [1d]の連立方程式を計算して、
 新しい時刻のHの分布を求める
 - [3] 時刻を進めて[1]に戻る

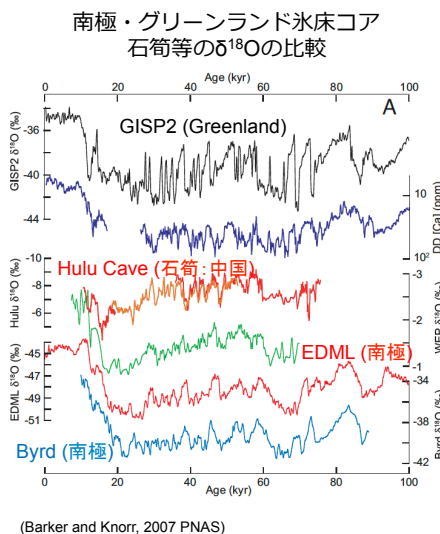
基本的にはこれだけ！！！

連立方程式はこんななかたち

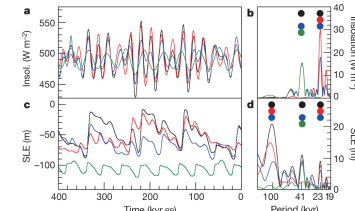
$$\begin{array}{l} \text{1番目の点} \quad b_1 \quad c_1 \quad 0 \quad \left(\begin{array}{c} H_1 \\ H_2 \\ \vdots \\ H_{n-1} \\ H_n \end{array} \right) = \left(\begin{array}{c} r_1 \\ r_2 \\ \vdots \\ r_{n-1} \\ r_n \end{array} \right) \\ \text{2番目の点} \quad a_2 \quad b_2 \quad c_2 \quad \left(\begin{array}{c} H_1 \\ H_2 \\ \vdots \\ H_{n-1} \\ H_n \end{array} \right) = \left(\begin{array}{c} r_1 \\ r_2 \\ \vdots \\ r_{n-1} \\ r_n \end{array} \right) \\ \vdots \\ \text{N番目の点} \quad 0 \quad a_n \quad b_{n-1} \quad c_{n-1} \quad \left(\begin{array}{c} H_1 \\ H_2 \\ \vdots \\ H_{n-1} \\ H_n \end{array} \right) = \left(\begin{array}{c} r_1 \\ r_2 \\ \vdots \\ r_{n-1} \\ r_n \end{array} \right) \end{array}$$

未知数：新しい時刻のH (N個ある)
 古い時刻のH

古環境プロキシデータの比較と数値モデルリング



数値モデルによる 過去40万年の北半球氷床の再現実験



Supplementary Video V1.

Simulated ice sheet change for the last 400 kyr with IcIES-MIROC model

(Abe-Ouchi et al., 2013 Nature)

グリーンランド氷床の最近の変化

Table 13.2 | Surface mass balance (SMB) and rates of change of SMB of the Greenland ice sheet, calculated from ice-sheet SMB models using meteorological observations and reanalyses as input, expressed as sea level equivalent (SLE). A negative SLE number for SMB indicates that accumulation exceeds runoff. A positive SLE for SMB anomaly indicates that accumulation has decreased, or runoff has increased, or both. Uncertainties are one standard deviation. Uncertainty in individual model results reflects temporal variability (1 standard deviations of annual mean values indicated); the uncertainty in the model average is 1 standard deviation of variation across models.

| Reference and Model ^a | Time-Mean SMB 1961–1990 mm yr ⁻¹ SLE | Rate of Change of SMB 1991–2010 mm yr ⁻² SLE | Time-Mean SMB Anomaly (With Respect to 1961–1990 Time-Mean SMB) ^b mm yr ⁻¹ SLE | | |
|--|---|---|--|-------------|-------------|
| | | | 1971–2010 | 1993–2010 | 2005–2010 |
| RACMO2, Van Angelen et al. (2012), 11 km RCM | -1.13 ± 0.30 | 0.04 ± 0.01 | 0.07 ± 0.33 | 0.23 ± 0.30 | 0.47 ± 0.24 |
| MAR, Fettweis et al. (2011), 25 km RCM | -1.17 ± 0.31 | 0.05 ± 0.01 | 0.12 ± 0.38 | 0.36 ± 0.33 | 0.64 ± 0.22 |
| PMMS, Box et al. (2009), 25 km RCM | -0.98 ± 0.18 | 0.02 ± 0.01 | 0.00 ± 0.19 | 0.10 ± 0.22 | 0.23 ± 0.21 |
| ECMWFd, Hanna et al. (2011), 5 km PDD | -0.77 ± 0.27 | 0.02 ± 0.01 | 0.02 ± 0.28 | 0.12 ± 0.27 | 0.24 ± 0.19 |
| SnowModel, Mernild and Liston (2012), 5 km EBM | -0.54 ± 0.21 | 0.03 ± 0.01 | 0.09 ± 0.25 | 0.19 ± 0.24 | 0.36 ± 0.23 |
| Model Average | -0.92 ± 0.26 | 0.03 ± 0.01 | 0.06 ± 0.05 | 0.20 ± 0.10 | 0.39 ± 0.17 |

Notes:

^a The approximate spatial resolution is stated and the model type denoted by PDD = positive degree day, EBM = Energy Balance Model, RCM = Regional Climate Model.

^b Difference from the time-mean SMB of 1961–1990. This difference equals the sea level contribution from Greenland SMB changes if the ice sheet is assumed to have been near zero mass balance during 1961–1990 (Hanna et al., 2005; Sasgen et al., 2012).

グリーンランドにおける変化



Figure 12. Ice evolution in Tasmeritut Fjord, southern Greenland, between 2009 and 2015. Note that retreat of Tasmeritut (red arrow) from a marine to a terrestrial terminus. The red star in the red box on the inset map denotes the location of the fjord. Image courtesy of Mauri Pelto/American Geophysical Union.

グリーンランド氷床の最近の変化

表面質量収支(質量の変化)=積雪量-表面融解量

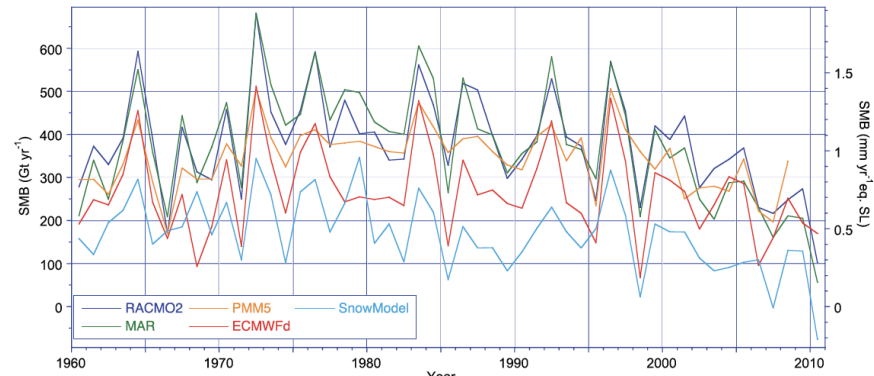
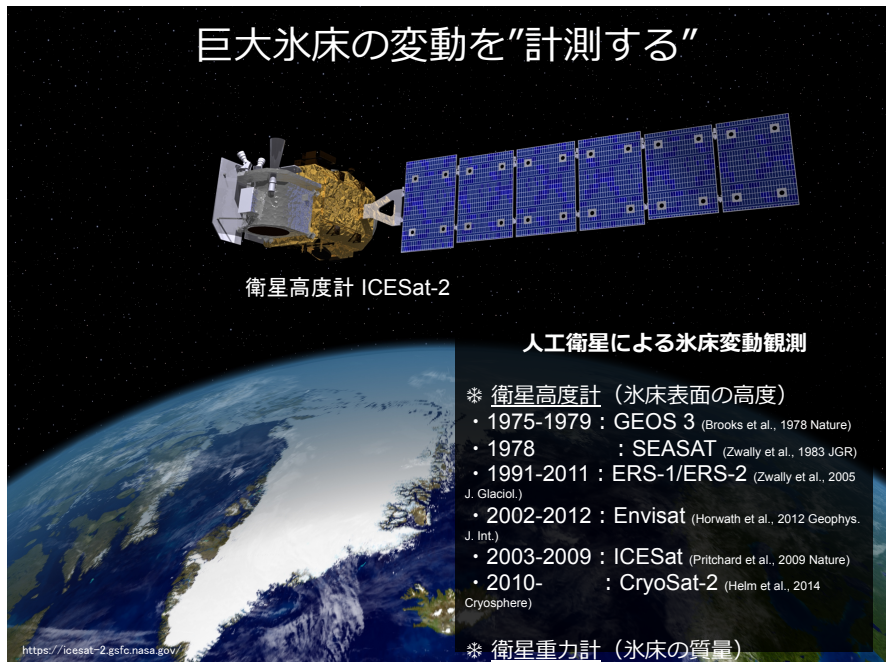


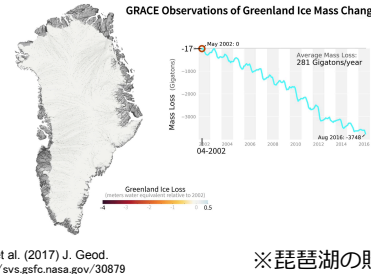
Figure 13.5 | Annual mean surface mass balance (accumulation minus ablation) for the Greenland ice sheet, simulated by five regional climate models for the period 1960–2010.

巨大氷床の変動を“計測する”

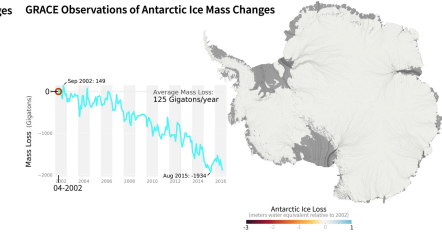


グリーンランド / 南極氷床の質量変動(2002-2016年)

グリーンランド氷床



南極氷床



※琵琶湖の貯水量 : 27.5 Gt

1993-2010: -121±28 Gt / year
2005-2010: -229±61 Gt / year
(IPCC, 2013)

1993-2010: -97±28 Gt / year
2005-2010: -147±61 Gt / year
(IPCC, 2013)

- 過去にはどのような氷床変動があったか？
- 氷床変動と、気候・海洋環境変動との関わりは？
- 将来はどのように変動するのか？

南極の最近の変化

IMBIE team, 2018 6月14日号, Nature

有意な質量減少が観測されている。

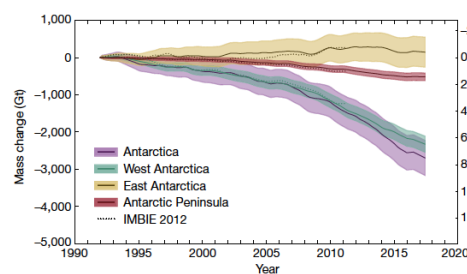
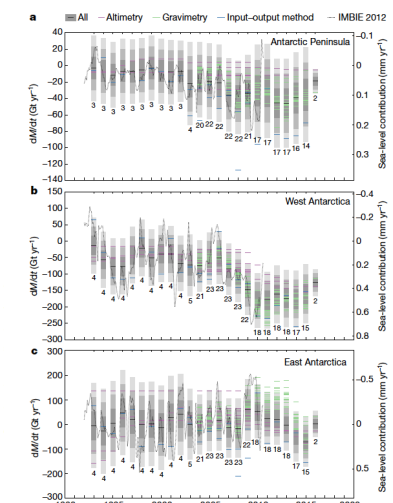


Table 1 | Rates of ice-sheet mass change

| | 1992-1997 (Gt yr ⁻¹) | 1997-2002 (Gt yr ⁻¹) | 2002-2007 (Gt yr ⁻¹) | 2007-2012 (Gt yr ⁻¹) | 2012-2017 (Gt yr ⁻¹) |
|------|----------------------------------|----------------------------------|----------------------------------|----------------------------------|----------------------------------|
| EIS | 11 ± 58 | 8 ± 56 | 12 ± 43 | 23 ± 38 | -28 ± 30 |
| WAIS | -53 ± 29 | -41 ± 28 | -65 ± 27 | -148 ± 27 | -159 ± 26 |
| APNS | -53 ± 13 | -4 ± 13 | -20 ± 13 | -31 ± 17 | -33 ± 16 |
| AIS | -49 ± 67 | -38 ± 64 | -72 ± 53 | -160 ± 50 | -219 ± 43 |

Rates were determined from all satellite measurements over various epochs for the EIS, WAIS and APNS, which combined constraints on AIS. The previous assessment¹⁵, which reported mass-balance estimates of 14 ± 43 Gt yr⁻¹ for the EIS, -65 ± 26 Gt yr⁻¹ for the WAIS, -29 ± 14 Gt yr⁻¹ small differences in our updated estimates for this period are due to our inclusion of more data. Errors are 1 σ .



20世紀の海面変動の要因別寄与

mm/yr

Table 13.1 | Global mean sea level budget (mm yr⁻¹) over different time intervals from observations and from model-based contributions. Uncertainties are 5 to 95%. The Atmosphere-Ocean General Circulation Model (AOGCM) historical integrations end in 2005; projections for RCP4.5 are used for 2006–2010. The modelled thermal expansion and glacier contributions are computed from the CMIP5 results, using the model of Marzeion et al. (2012a) for glaciers. The land water contribution is due to anthropogenic intervention only, not including climate-related fluctuations.

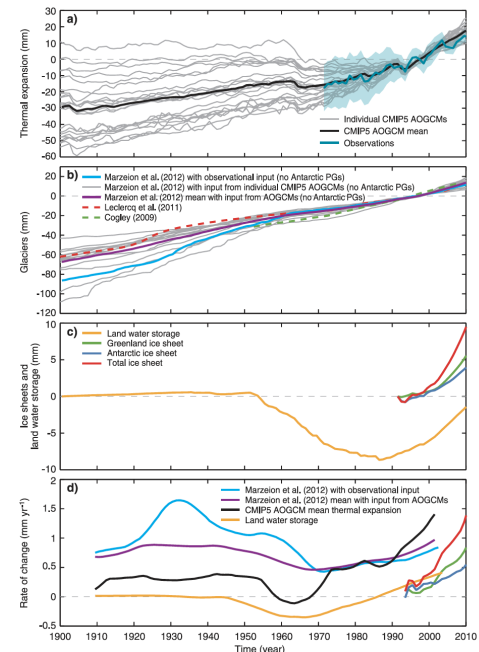
| Source | 1901–1990 | 1971–2010 | 1993–2010 |
|--|------------------------|---------------------|----------------------------------|
| Observed contributions to global mean sea level (GMSL) rise | | | |
| Thermal expansion | – | 0.8 [0.5 to 1.1] | 1.1 [0.8 to 1.4] |
| Glaciers except in Greenland and Antarctica ^a | 0.54 [0.47 to 0.61] | 0.62 [0.25 to 0.99] | 0.76 [0.39 to 1.13] |
| Glaciers in Greenland ^b | 0.15 [0.10 to 0.19] | 0.06 [0.03 to 0.09] | 0.10 [0.07 to 0.13] ^b |
| Greenland ice sheet | – | – | 0.33 [0.25 to 0.41] |
| Antarctic ice sheet | – | – | 0.27 [0.16 to 0.38] |
| Land water storage | -0.11 [-0.16 to -0.06] | 0.12 [0.03 to 0.22] | 0.38 [0.26 to 0.49] |
| Total of contributions | – | – | 2.8 [2.3 to 3.4] |
| Observed GMSL rise | 1.5 [1.3 to 1.7] | 2.0 [1.7 to 2.3] | 3.2 [2.8 to 3.6] |
| Modelled contributions to GMSL rise | | | |
| Thermal expansion | 0.37 [0.06 to 0.67] | 0.96 [0.51 to 1.41] | 1.49 [0.97 to 2.02] |
| Glaciers except in Greenland and Antarctica | 0.63 [0.37 to 0.89] | 0.62 [0.41 to 0.84] | 0.78 [0.43 to 1.13] |
| Glaciers in Greenland | 0.07 [-0.02 to 0.16] | 0.10 [0.05 to 0.15] | 0.14 [0.06 to 0.23] |
| Total including land water storage | 1.0 [0.5 to 1.4] | 1.8 [1.3 to 2.3] | 2.8 [2.1 to 3.5] |
| Residual ^c | 0.5 [0.1 to 1.0] | 0.2 [-0.4 to 0.8] | 0.4 [-0.4 to 1.2] |

Notes:

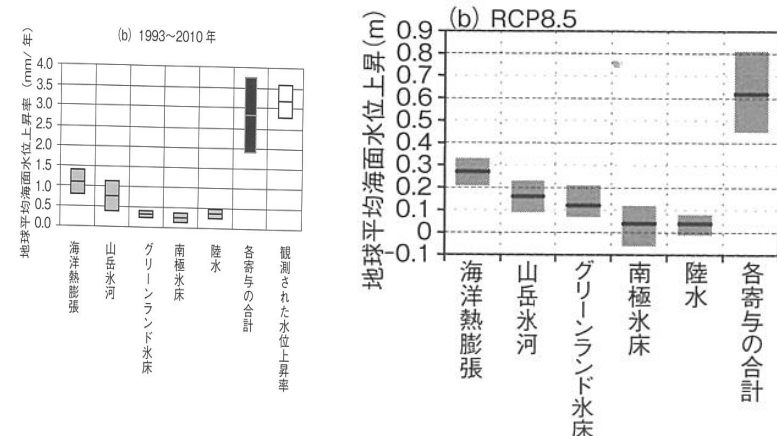
a: Data for all glaciers extend to 2009, not 2010.

b: This contribution is not included in the total because glaciers in Greenland are included in the observational assessment of the Greenland ice sheet.

c: Observed GMSL rise – modelled thermal expansion – modelled glaciers – observed land water storage

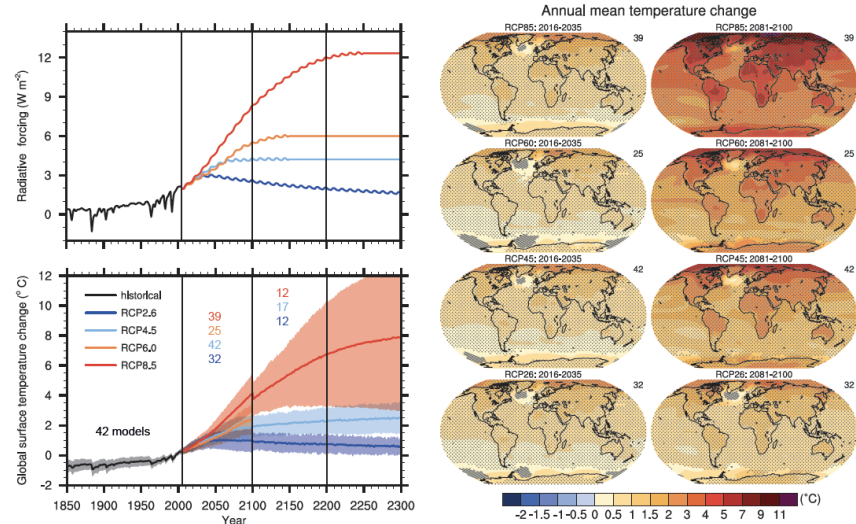


最近の海面変化と将来予測 (AR5, 気象学会、朝倉書店、2014)

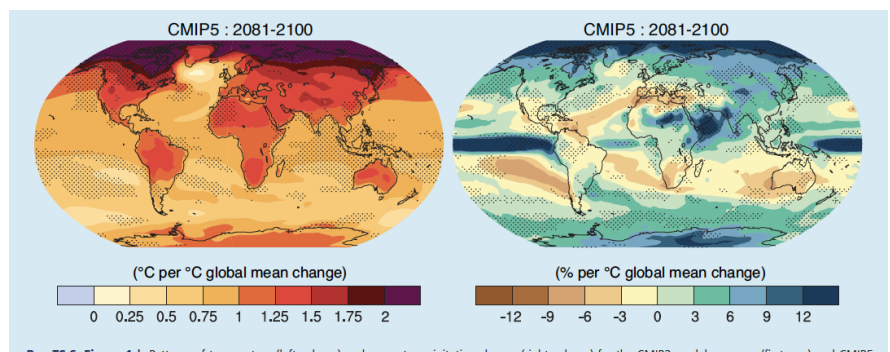


放射強制力と気温の将来予測(AR5)

シナリオ別、1850 ~ 2100 and 2300、マルチモデルAOGCM結果

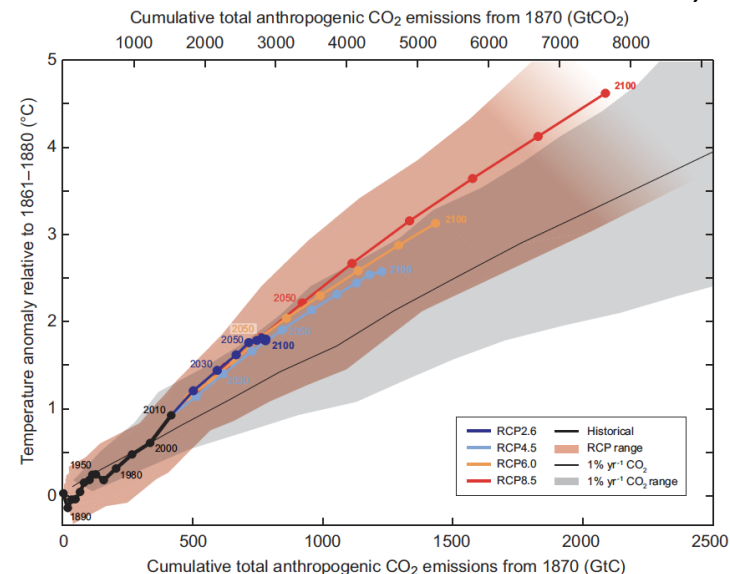


気温と降水量変化(AR5)



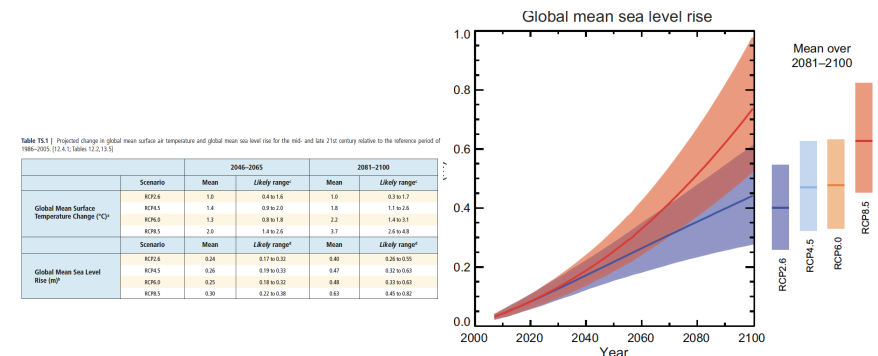
Box TS.6, Figure 1 | Patterns of temperature (left column) and percent precipitation change (right column) for the CMIP3 models average (first row) and CMIP5

CO₂排出量と気温将来予測比較(AR5)

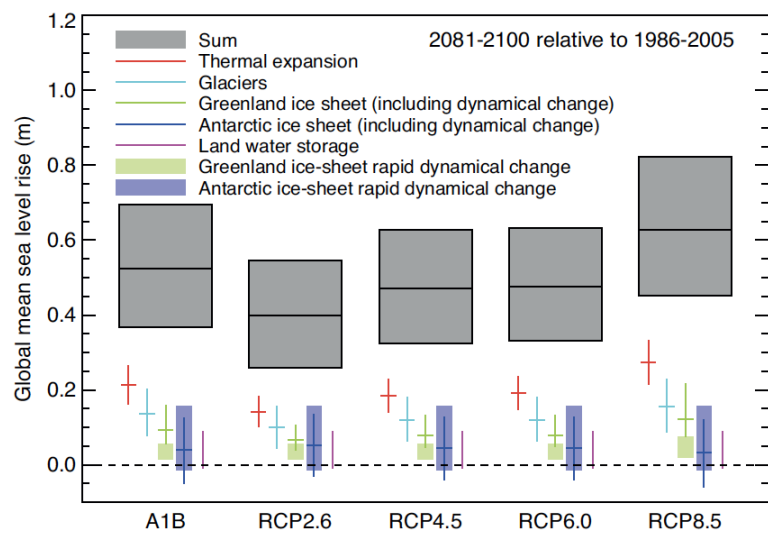


海面上昇の将来予測(AR5)

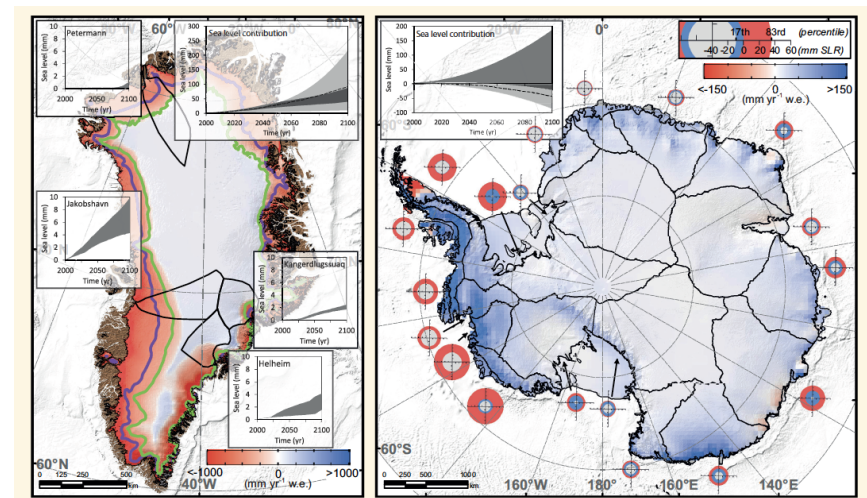
Global mean sea level will continue to rise during the 21st century (see Figure SPM.9). Under all RCP scenarios, the rate of sea level rise will very likely exceed that observed during 1971 to 2010 due to increased ocean warming and increased loss of mass from glaciers and ice sheets. (13.3–13.5)



シナリオごとの海面上昇AR5予測



表面質量収支と氷床流出の21世紀末までの変化 (南極A1B, グリーンランドRCP4.5)



21世紀末までの全球海面変化予測 (AR5)

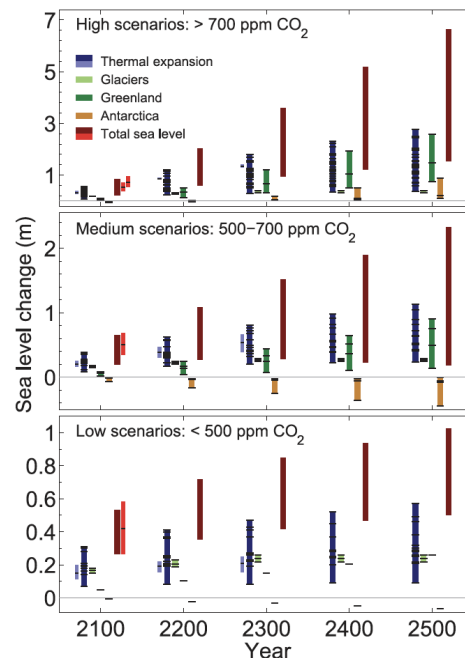
Table 13.5 | Median values and *likely* ranges for projections of global mean sea level (GMSL) rise and its contributions in metres in 2081–2100 relative to 1986–2005 for the four RCP scenarios and SRES A1B, GMSL rise in 2046–2065 and 2100, and rates of GMSL rise in mm yr⁻¹ in 2081–2100. See Section 13.5.1 concerning how the *likely* range is defined.

| | SRES A1B | RCP2.6 | RCP4.5 | RCP6.0 | RCP8.5 |
|---|------------------------|------------------------|------------------------|------------------------|------------------------|
| Thermal expansion | 0.21 [0.16 to 0.26] | 0.14 [0.10 to 0.18] | 0.19 [0.14 to 0.23] | 0.19 [0.15 to 0.24] | 0.27 [0.21 to 0.33] |
| Glaciers ^a | 0.14 [0.08 to 0.21] | 0.10 [0.04 to 0.16] | 0.12 [0.06 to 0.19] | 0.12 [0.06 to 0.19] | 0.16 [0.09 to 0.23] |
| Greenland ice-sheet SMB ^b | 0.05 [0.02 to 0.12] | 0.03 [0.01 to 0.07] | 0.04 [0.01 to 0.09] | 0.04 [0.01 to 0.09] | 0.07 [0.03 to 0.16] |
| Antarctic ice-sheet SMB ^b | -0.03 [-0.06 to -0.01] | -0.02 [-0.04 to -0.00] | -0.02 [-0.05 to -0.01] | -0.02 [-0.05 to -0.01] | -0.04 [-0.07 to -0.01] |
| Greenland ice-sheet rapid dynamics | 0.04 [0.01 to 0.06] | 0.05 [0.02 to 0.07] |
| Antarctic ice-sheet rapid dynamics | 0.07 [-0.01 to 0.16] |
| Land water storage | 0.04 [-0.01 to 0.09] |
| Global mean sea level rise in 2081–2100 | 0.52 [0.37 to 0.69] | 0.40 [0.26 to 0.55] | 0.47 [0.32 to 0.63] | 0.48 [0.33 to 0.63] | 0.63 [0.45 to 0.82] |
| Greenland ice sheet | 0.09 [0.05 to 0.15] | 0.06 [0.04 to 0.10] | 0.08 [0.04 to 0.13] | 0.08 [0.04 to 0.13] | 0.12 [0.07 to 0.21] |
| Antarctic ice sheet | 0.04 [-0.05 to 0.13] | 0.05 [-0.03 to 0.14] | 0.05 [-0.04 to 0.13] | 0.05 [-0.04 to 0.13] | 0.04 [-0.06 to 0.12] |
| Ice-sheet rapid dynamics | 0.10 [0.03 to 0.19] | 0.12 [0.03 to 0.20] |
| Rate of global mean sea level rise | 8.1 [5.1 to 11.4] | 4.4 [2.0 to 6.8] | 6.1 [3.5 to 8.8] | 7.4 [4.7 to 10.3] | 11.2 [7.5 to 15.7] |
| Global mean sea level rise in 2046–2065 | 0.27 [0.19 to 0.34] | 0.24 [0.17 to 0.32] | 0.26 [0.19 to 0.33] | 0.25 [0.18 to 0.32] | 0.30 [0.22 to 0.38] |
| Global mean sea level rise in 2100 | 0.60 [0.42 to 0.80] | 0.44 [0.28 to 0.61] | 0.53 [0.36 to 0.71] | 0.55 [0.38 to 0.73] | 0.74 [0.52 to 0.98] |

Only the collapse of the marine-based sectors of the Antarctic ice sheet, if initiated, could cause GMSL to rise substantially above the *likely* range during the 21st century. This potential additional contribution cannot be precisely quantified but there is medium confidence that it would not exceed several tenths of a meter of sea level rise.

長期予測 500年後?

気候モデルによる海洋温度、
氷河氷床の表面質量収支変化
などを考慮。
(南極氷床の力学効果が入って
いないことに注意)



Semi empirical modelによる予測

| | From | To | 5% | 50% | 95% |
|--|-----------|-----------|------|------|------|
| Scenario SRES A1B | | | | | |
| IPCC AR4 ^a | 1990 | 2100 | 0.22 | 0.37 | 0.50 |
| IPCC AR4 ^{a,b} | 1990 | 2100 | 0.22 | 0.43 | 0.65 |
| IPCC AR5 (also in Table 13.5) | 1996 | 2100 | 0.42 | 0.60 | 0.80 |
| Rahmstorf (2007) ^a | 1990 | 2100 | — | 0.85 | — |
| Horton et al. (2008) ^a | 2000 | 2100 | 0.62 | 0.74 | 0.88 |
| Vermeer and Rahmstorf (2009) | 1990 | 2100 | 0.98 | 1.24 | 1.56 |
| Grinsted et al. (2010) with Brohan et al. (2006) temperature for calibration | 1990 | 2100 | 0.32 | 0.83 | 1.34 |
| Grinsted et al. (2010) with Moberg et al. (2005) temperature for calibration | 1990 | 2100 | 0.91 | 1.12 | 1.32 |
| Jevrejeva et al. (2010) with Crowley et al. (2003) forcing for calibration | 1990 | 2100 | 0.63 | 0.86 | 1.06 |
| Jevrejeva et al. (2010) with Goosse et al. (2005) forcing for calibration | 1990 | 2100 | 0.60 | 0.75 | 1.15 |
| Jevrejeva et al. (2010) with Tett et al. (2007) forcing for calibration | 1990 | 2100 | 0.87 | 1.15 | 1.40 |
| Scenario RCP4.5 | | | | | |
| IPCC AR5 (also in Table 13.5) | 1986–2005 | 2081–2100 | 0.32 | 0.47 | 0.63 |
| Grinsted et al. (2010) calibrated with Moberg et al. (2005) temperature | 1986–2005 | 2081–2100 | 0.63 | 0.88 | 1.14 |
| Rahmstorf et al. (2012b) calibrated with Church and White (2006) GMSL | 1986–2005 | 2081–2100 | 0.79 | 0.86 | 0.93 |
| Rahmstorf et al. (2012b) calibrated with Church and White (2011) GMSL | 1986–2005 | 2081–2100 | 0.57 | 0.63 | 0.68 |
| Rahmstorf et al. (2012b) calibrated with Jevrejeva et al. (2008) GMSL | 1986–2005 | 2081–2100 | 0.82 | 0.97 | 1.12 |
| Rahmstorf et al. (2012b) calibrated with proxy data | 1986–2005 | 2081–2100 | 0.56 | 0.88 | 1.24 |
| Jevrejeva et al. (2012a) calibrated with Goosse et al. (2005) radiative forcing | 1986–2005 | 2081–2100 | 0.43 | 0.56 | 0.69 |
| Jevrejeva et al. (2012a) calibrated with Crowley et al. (2003) radiative forcing | 1986–2005 | 2081–2100 | 0.48 | 0.65 | 0.80 |

長期予測と 古気候

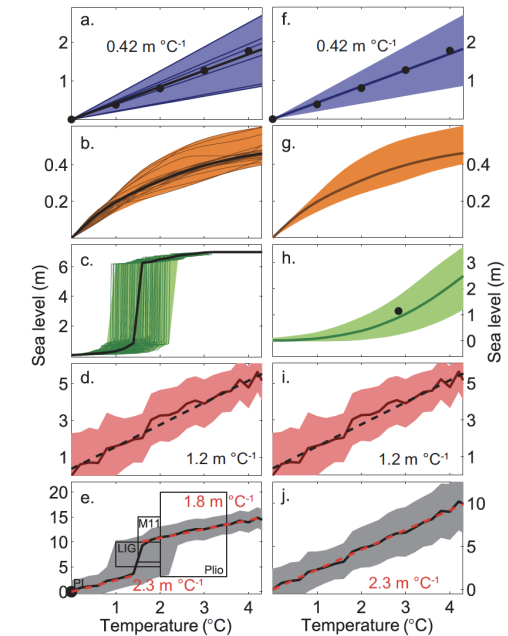


Figure 13.14 | (Left column) Multi-millennial sea level commitment per degree Celsius of warming as obtained from physical model simulations of (a)

海面の 地域的変化 20世紀まで

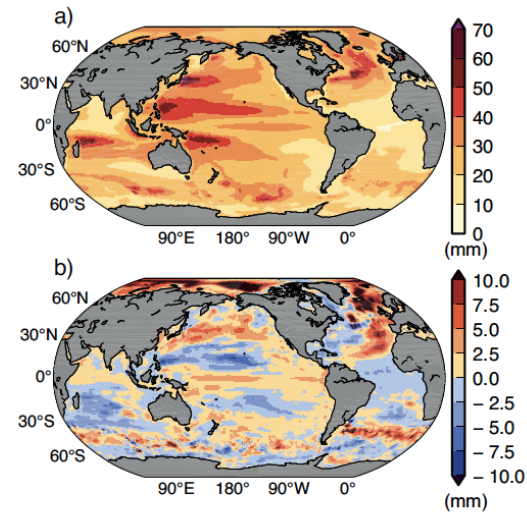


Figure 13.15 | (a) Root-mean square (RMS) interannual dynamic sea level variability (millimetres) in a CMIP5 multi-model ensemble (21 models), built from the historically forced experiments during the period 1951–2005. (b) Changes in the ensemble average interannual dynamic sea level variability (standard deviation (SD), in millimetres) evaluated over the period 2081–2100 relative to the reference period 1986–2005. The projection data (2081–2100) are from the CMIP5 RCP4.5 experiment.

21世紀末海面の地域的变化予測

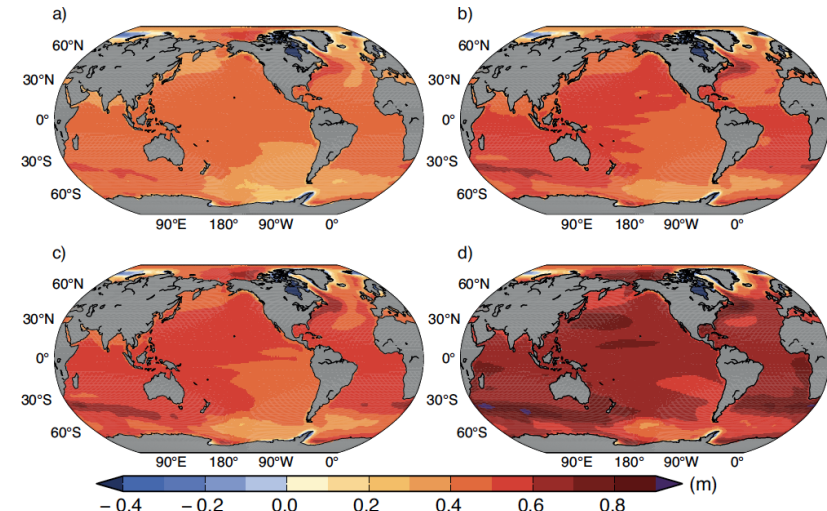
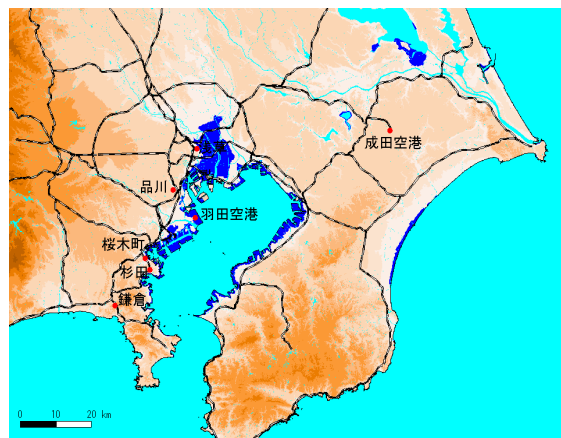


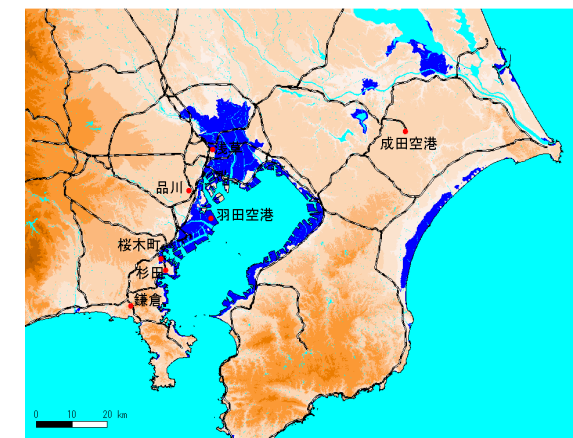
Figure 13.20 | Ensemble mean regional relative sea level change (metres) evaluated from 21 CMIP5 models for the RCP scenarios (a) 2.6, (b) 4.5, (c) 6.0 and (d) 8.5 between 1986–2005 and 2081–2100. Each map includes effects of atmospheric loading, plus land ice, glacial isostatic adjustment (GIA) and terrestrial water sources.

Sea level influence of 1m 海水準 1 m 上昇の浸水域



北海道地図株式会社のGISMAPを使用

Sea level influence of 3 m 海水準 3 m 上昇の浸水域



北海道地図株式会社のGISMAPを使用

海面上昇 50cm による洪水頻度の増加

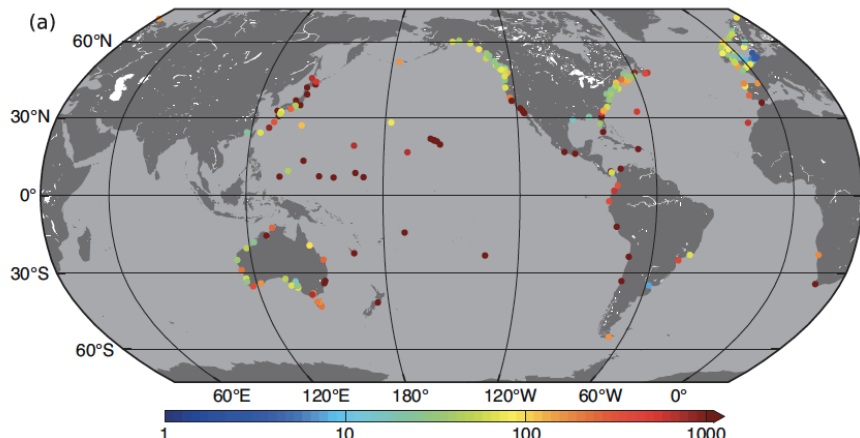
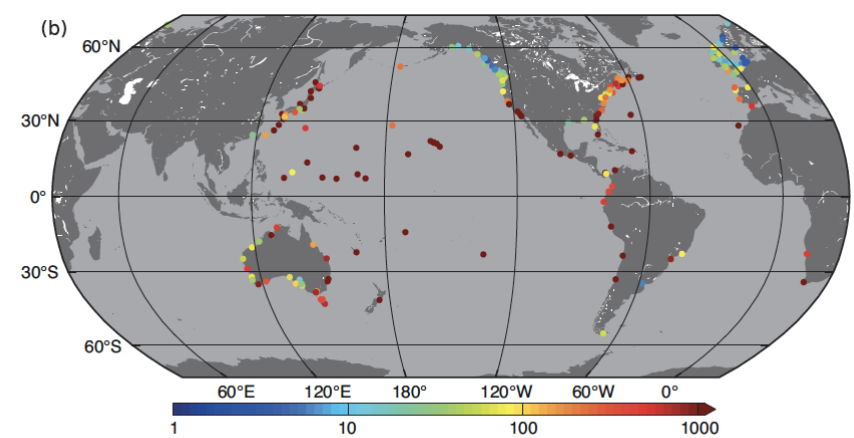


Figure 13.25 | The estimated multiplication factor (shown at tide gauge locations by colored dots), by which the frequency of flooding events of a given height increase for (a) a mean sea level (MSL) rise of 0.5 m (b) using regional projections of MSL for the RCP4.5 scenario, shown in Figure 13.19a.

海面上昇 RCP4.5 による洪水頻度の増加



5 | The estimated multiplication factor (shown at tide gauge locations by colored dots), by which the frequency of flooding events of a given height increase for (b) a mean sea level (MSL) rise of 0.5 m using regional projections of MSL for the RCP4.5 scenario, shown in Figure 13.19a.

まとめ

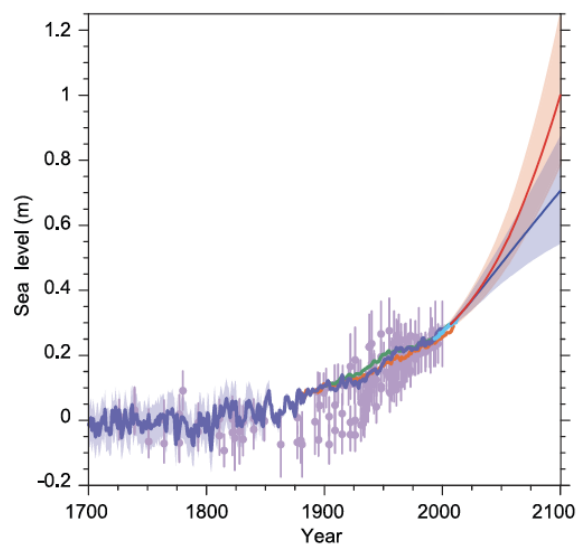
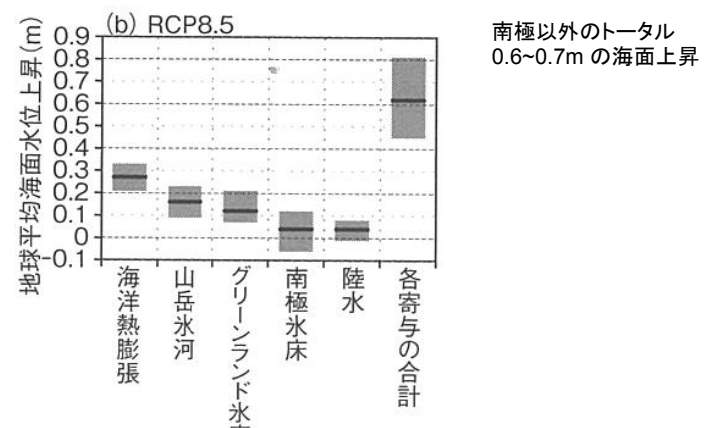
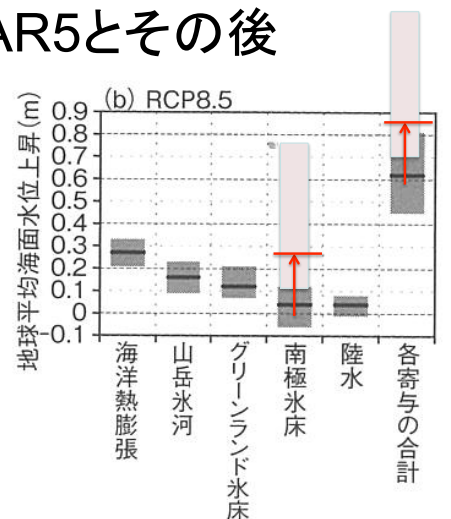


Figure 13.27 | Compilation of paleo sea level data, tide gauge data, altimeter data (from Figure 13.3), and central estimates and likely ranges for projections of global mean sea level rise for RCP2.6 (blue) and RCP8.5 (red) scenarios (Section 13.5.1), all relative to pre-industrial values.

RCP8.5の21世紀の海面上昇： AR5



RCP8.5の21世紀の海面上昇: AR5とその後



南極以外のトータル
0.6~0.7m の海面上昇

——>
南極の寄与が
AR5後の研究により
0.18~0.79 (0.35に修正)
= 約0.25

つまり、
21C末に 62cm 上昇
の予測が、85cm に
上方修正

南極氷床の寄与

- Based on current understanding, only the collapse of marine-based sectors of the Antarctic ice sheet, if initiated, could cause global mean sea level to rise substantially above the *likely* range during the 21st century. However, there is *medium confidence* that this additional contribution would not exceed several tenths of a meter of sea level rise during the 21st century. [13.4, 13.5]

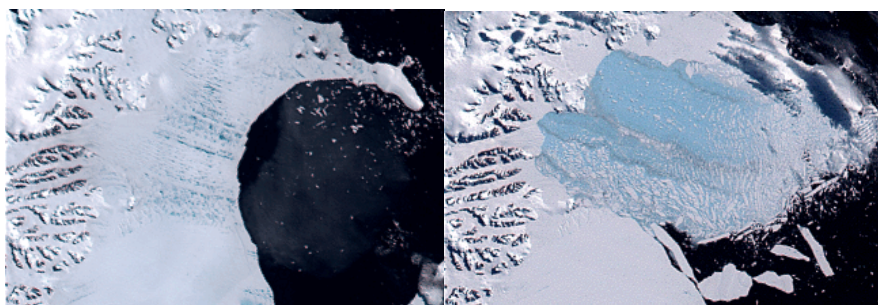
予測を大きく上回るとしたら、南極氷床の海洋着床部分の崩壊がある場合だけだ。
しかし、21C中に50cm以上ということはない。

Some observation of rapid retreat of ice shelf and fast flow of ice stream in West Antarctica

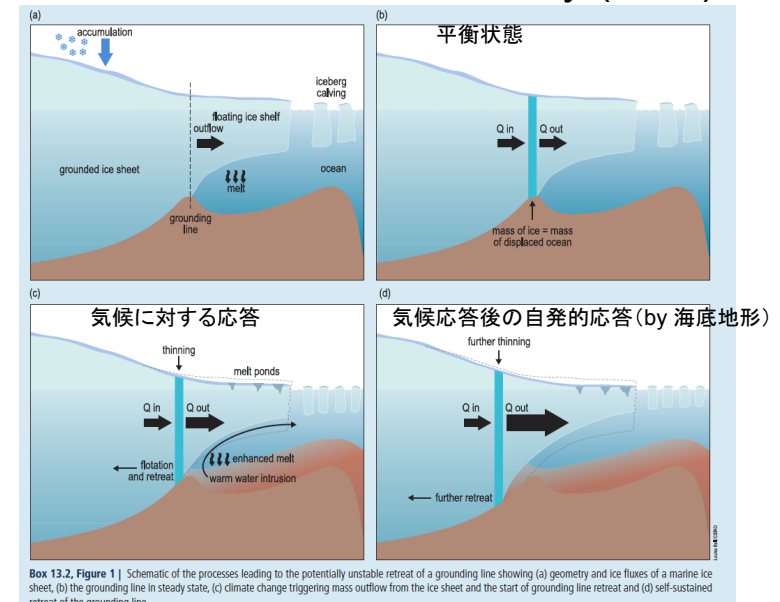
(Larsen Ice Shelf)

西南極：棚氷や水流の急速な消失が一部観測される

- 南極半島のLarsen 棚氷が数ヶ月で3250km²が消失した。(衛星写真MODIS, <http://wwwnsidc.colorado.edu/sotc/iceshelves.html>)
- 温暖化により棚氷消失がすむと西南極氷床の力学的不安定をもたらすのでは？という説があるが、数値モデル化も観測も不足していて今後の研究課題となっている。



Marine ice sheet instability (MISI)



南極氷床の不確実性

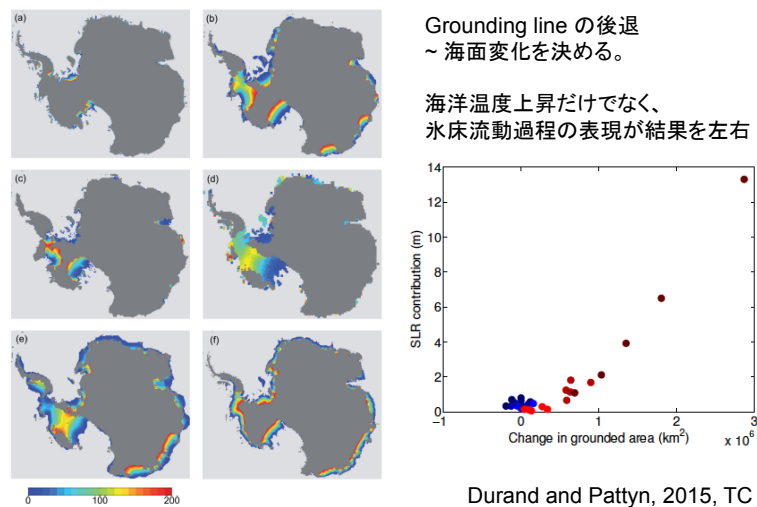
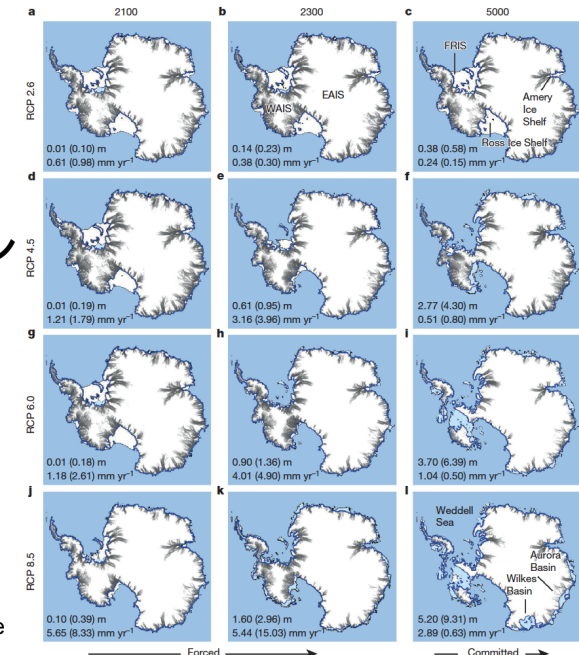


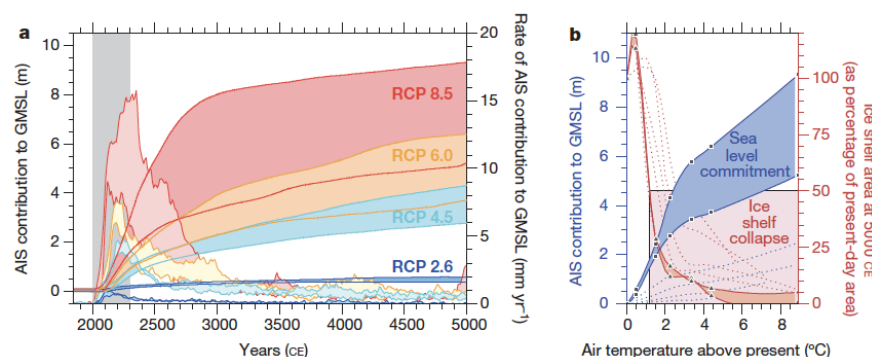
Figure 2. Evolution of the Antarctic grounded area as computed by the five models which participated to SeaRISE experiment M3 (a to e) and similar results obtained by SISM (f). Colors corresponds to the time of ungrounding.

南極氷床の 温暖化に対 する応答シ ミュレーション



Golledge et al, 2015, Nature

南極氷床の 温暖化に対 する応答シ ミュレーション



南極氷床の 温暖化に対 する応答シ ミュレーション (2)

DeConte and Pollard, 2016, Nature

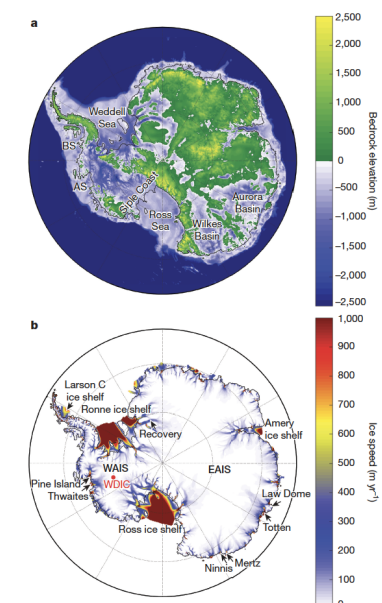
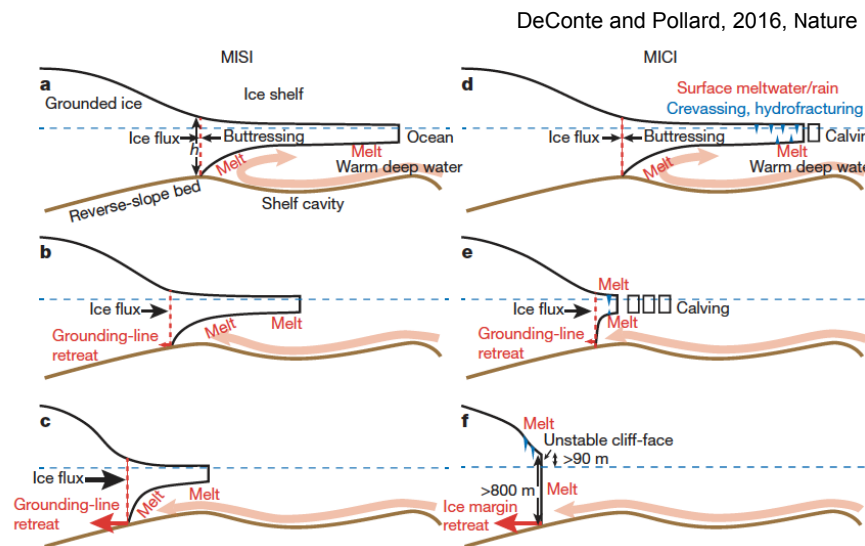


Figure 5 | Antarctic sub-glacial topography and ice sheet features. a, Bedrock elevations¹³ interpolated onto the 10-km polar stereographic ice-sheet model grid and used in Pliocene, LIG, and future ice-sheet simulations. b, Model surface ice speeds and grounding lines (black lines)

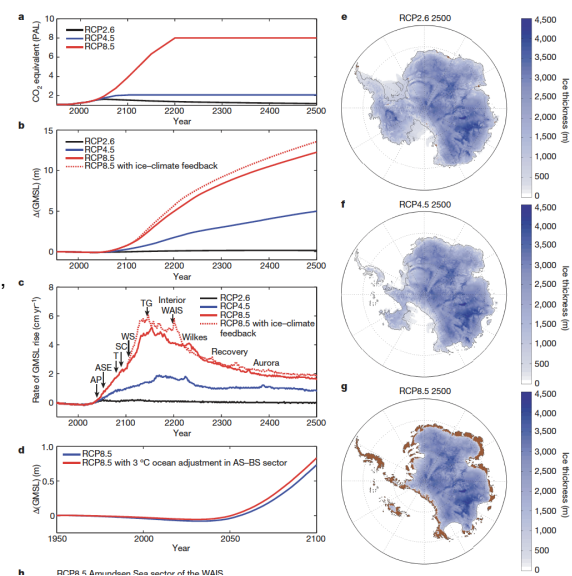
南極氷床におけるMISIとMICI

Marine Ice Sheet instability and Marine Ice Cliff instability



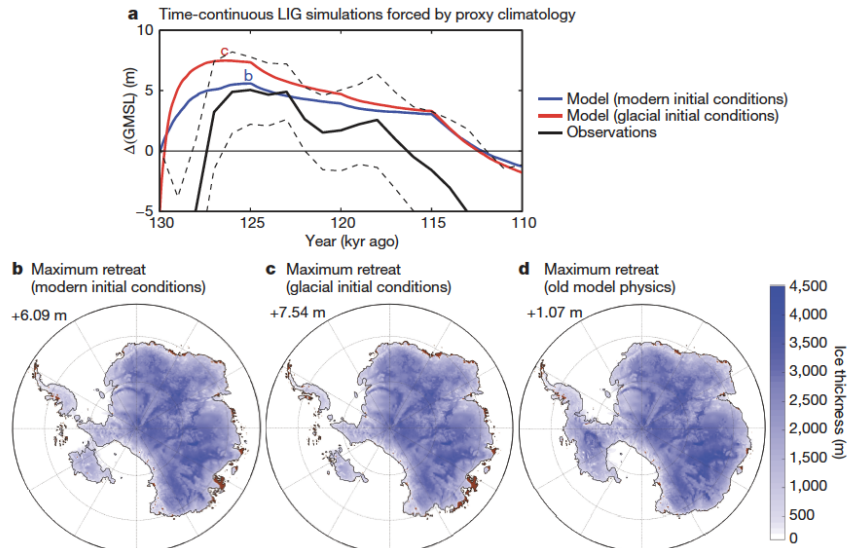
南極氷床の 温暖化に対する応答シミュレーション

DeConte and Pollard, 2016, Nature



南極氷床モデル変化の古気候変化による制約

DeConte and Pollard, 2016, Nature



南極氷床の温暖化に対する応答 シミュレーション

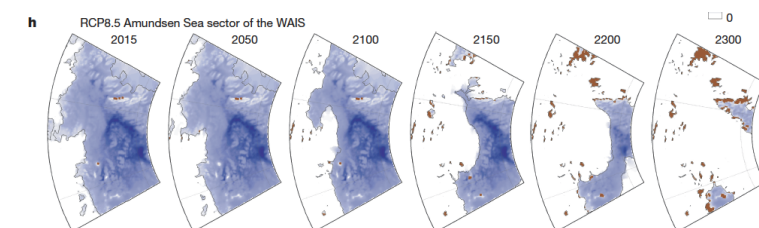
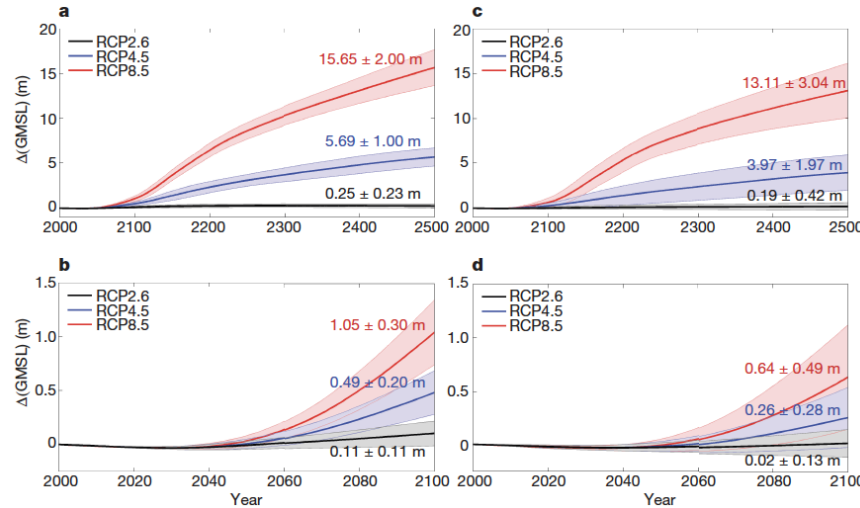


Figure 4 | Future ice-sheet simulations and Antarctic contributions to GMSL from 1950 to 2500 driven by a high-resolution atmospheric model and 1° NCAR CCSM4 ocean temperatures. a, Equivalent CO₂ forcing applied to the simulations, following the RCP emission scenarios in ref. 36, except limited to 8 × PAL (preindustrial atmospheric level, where 1 PAL = 280 p.m.v.). b, Antarctic contribution to GMSL. c, Rate of sea-level rise and approximate timing of major retreat and thinning in the Antarctic Peninsula (AP), Amundsen Sea Embayment (ASE) outlet glaciers, AS-BS, Amundsen Sea–Bellingshausen Sea; the Totten (T), Siple Coast (SC) and Weddell Sea (WS) grounding zones, the deep Thwaites Glacier basin (TG), Interior WAIS, the Recovery Glacier, and the deep EAIS basins (Wilkes and Aurora). d, Antarctic contribution to GMSL over the next 100 years for RCP8.5 with and without a +3°C adjustment in ocean model temperatures in the Amundsen and Bellingshausen seas as shown in Extended Data Fig. 5d. e–g, Ice-sheet snapshots at 2500 in the RCP2.6 (e), RCP4.5 (f) and RCP8.5 (g) scenarios. Ice-free land surfaces are shown in brown. h, Close-ups of the Amundsen Sea sector of WAIS in RCP8.5 with bias-corrected ocean model temperatures.

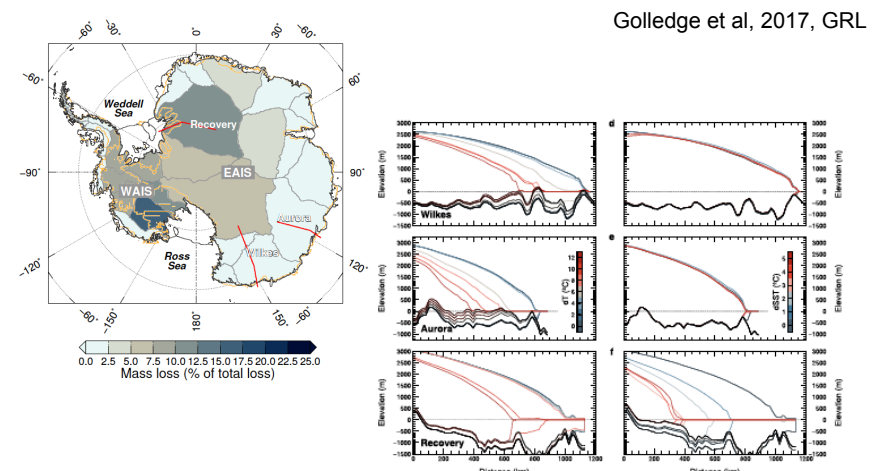
DeConte and Pollard, 2016, Nature

南極氷床の温暖化に対する応答



DeConte and Pollard, 2016, Nature

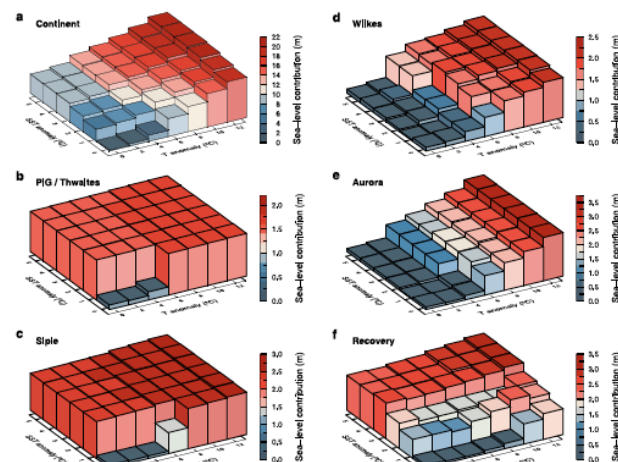
南極氷床の温度に対する応答実験



Figures 2. Transsects through these major East Antarctic drainage basins after 10,000 model years (see Figure S3 for locations). (a-c) All three investigated sectors of East Antarctica respond to atmospheric warming by retreating inland. However, the magnitude of warming required to initiate retreat, as well as the rate of recession, are dictated by local topography and ice sheet configuration. (d-f) In the absence of atmospheric warming, only Recovery Glacier retreats in response to a warming ocean. Glaciers in both Wilkes and Aurora subglacial basins remain stable due to the greater thickness of ice above flotation at their present-day grounding lines. Panels also show bedrock uplift following ice retreat.

南極氷床の温度に対する応答実験

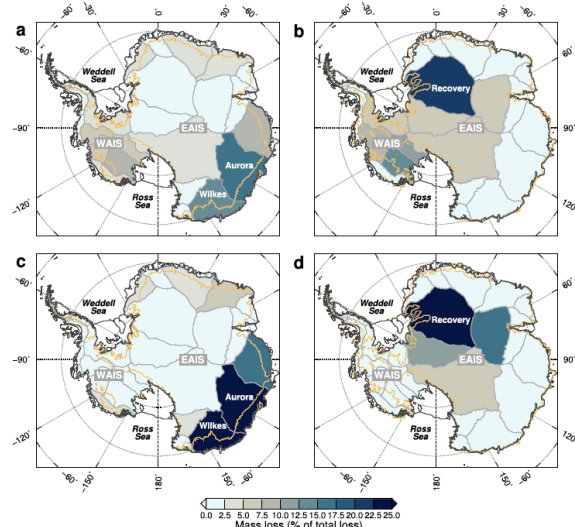
地域によって大気に対する応答と海洋に対する応答が異なることを表す



Figures 1. (a) Continent-wide sea-level contributions after 10,000 model years. (b-f) Sea-level contributions from five discrete drainage basins, showing considerable differences in environmental sensitivity and nature of threshold response under warmer-than-present air (T) and ocean (SST) temperatures. The Pine Island Glacier (PIG)/Thwaites Glacier and Siple Coast catchments of West Antarctica (Figures 1b and 1c) exhibit high sensitivity to relatively modest warming values; Wilkes (Figure 1d) and Aurora (Figure 1e) catchments exhibit a threshold sensitivity to air temperature, but not ocean temperature; Recovery basin (Figure 1f) exhibits an abrupt response to ocean temperature but is less sensitive to air temperature.

南極氷床の温度に対する応答実験

Figures 3. (a) Relative sensitivity of each Antarctic catchment to atmospheric forcing, based on the proportion of total ice loss arising with a spatially uniform air temperature increase of 2°C . Wilkes and Aurora basins exhibit by far the greatest response. (b) Relative sensitivity of Antarctic catchments to oceanic forcing, based on the proportion of total ice loss arising with a spatially uniform ocean temperature increase of 2°C . The greatest response is evident in Recovery basin. (c, d) As Figures 3a and 3b but with the ice loss effect of topography subtracted (see supporting information for details). Removing the topographic influence on ice loss highlights more clearly the spatial influence of air and ocean forcing. Orange lines denote grounding-line position at the time slice used for the mass loss calculations (10,000 years). WAIS = West Antarctic ice sheet; EAIS = East Antarctic ice sheet.



南極氷床周辺の海洋の温度の21世紀末の変化

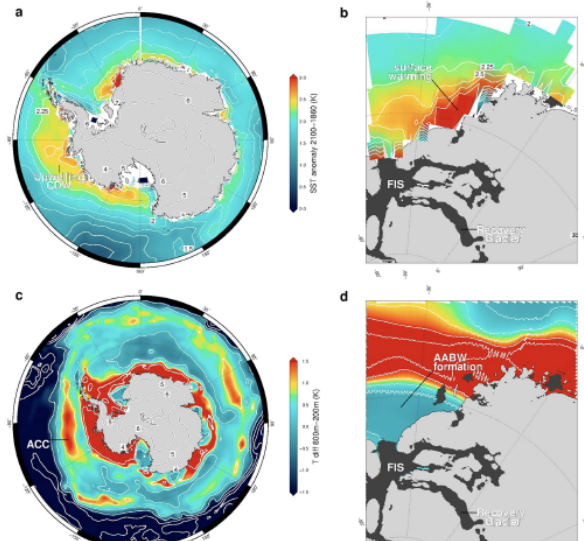
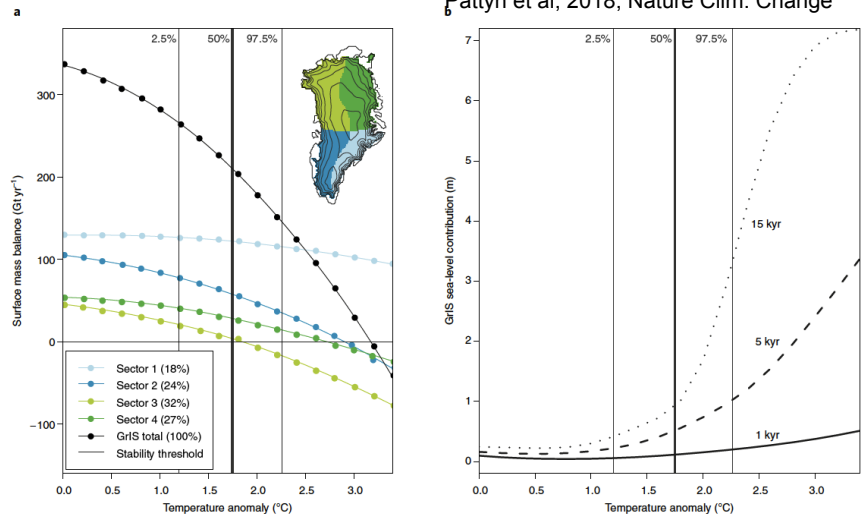


Figure 4 | (a) Sea-surface temperature anomalies at 2100 CE (colored shading) with respect to preindustrial values as represented in the CMIP5 ensemble mean. Note the widespread cooling associated with Antarctic bottom upwelling under polar deep water and (b) the patchy warming in the eastern Weddell Sea adjacent to the Midway Ice Shelf. (b) Vertical ocean temperature differences between the CMIP5 Simulation Experiment (CE) and the twentieth-century observation (PD). Bright colors in the Southern Ocean identify the location of the Antarctic Circumpolar Current. Areas of low thermal gradient adjacent to the continent coincide with the location of Antarctic Bottom Water formation areas, including (d) in the eastern Weddell Sea. Data shown are interpolations that fill gaps between available data points, for example, beneath ice shelves. Air temperature anomalies (in degrees C) over land shown as contours in Figures 4a and 4c. Dark gray shading in Figures 4b and 4d depicts areas of bad topography more than 500 m below sea level.

グリーンランド氷床の気温に対する応答



Robinson et al, 2012, Nature Clim. Change
Pattyn et al, 2018, Nature Clim. Change

氷床の気温に対する応答（表面の応答vs力学応答）

The Greenland and Antarctic ice sheets under 1.5 °C global warming

Frank Pattyn^{①*}, Catherine Ritz², Edward Hanna³, Xylar Asay-Davis^{④,5}, Rob DeConto⁶, Gaël Durand², Lionel Favier^{1,2}, Xavier Fettweis^⑦, Heiko Goelzer^{1,8}, Nicholas R. Golledge^{⑨,10}, Peter Kuipers Munneke⁹, Jan T. M. Lenaerts^⑩, Sophie Nowicki¹¹, Antony J. Payne¹², Alexander Robinson¹⁴, Hélène Seroussi¹³, Luke D. Trusel^⑪ and Michiel van den Broek^⑫

Even if anthropogenic warming were constrained to less than 2 °C above pre-industrial, the Greenland and Antarctic ice sheets will continue to lose mass, albeit with reduced rates of mass loss. However, nonlinear responses cannot be excluded, which may lead to larger rates of mass loss. Furthermore, large uncertainties in future projections still remain, pertaining to knowledge gaps in atmospheric (Greenland) and oceanic (Antarctica) forcing. On millennial timescales, both ice sheets have tipping points at or slightly above the 1.5–2.0 °C threshold; for Greenland, this may lead to irreversible mass loss due to the surface mass balance–elevation feedback, whereas for Antarctica, this could result in a collapse of major drainage basins due to ice-shelf weakening.

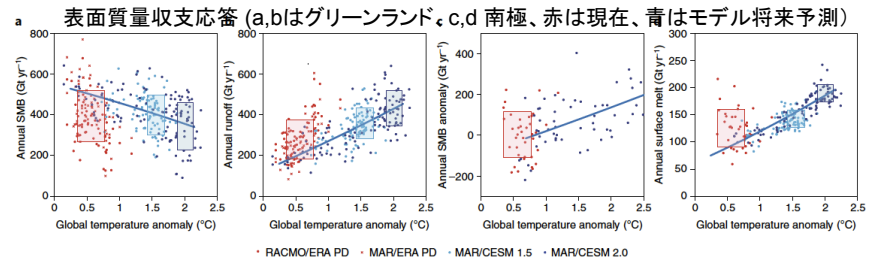


Fig. 1 | Annual mean surface mass fluxes as a function of global mean temperature anomalies. Temperature anomalies are referenced to the pre-industrial era (1850–1920). **a**, GrIS SMB. **b**, GrIS runoff. **c**, Antarctic SMB. **d**, Antarctic surface melt. Red colours indicate model realizations of present-day ice sheets (RACMO2 and MAR forced by ERA reanalysis data). Blue colours indicate model realizations of future ice sheets. In **a** and **b**, MAR is forced with CESM-

南極氷床の気温に対する応答

Golledge et al, 2015, Nature
Pattyn et al, 2018, Nature Clim. Change

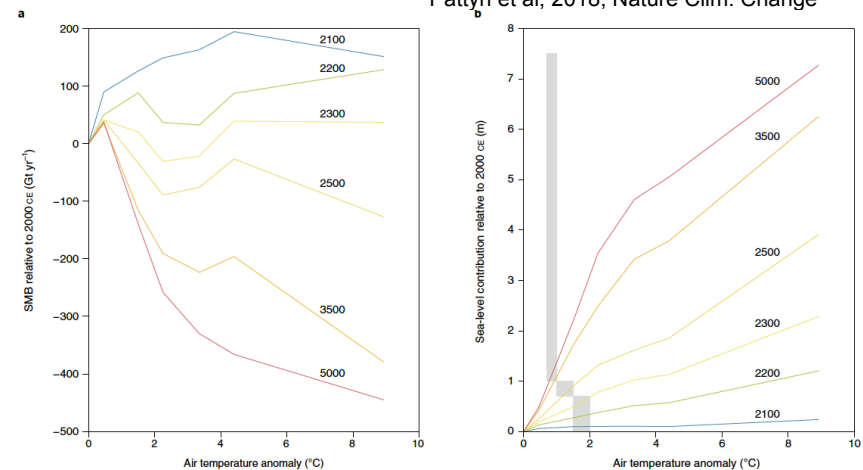
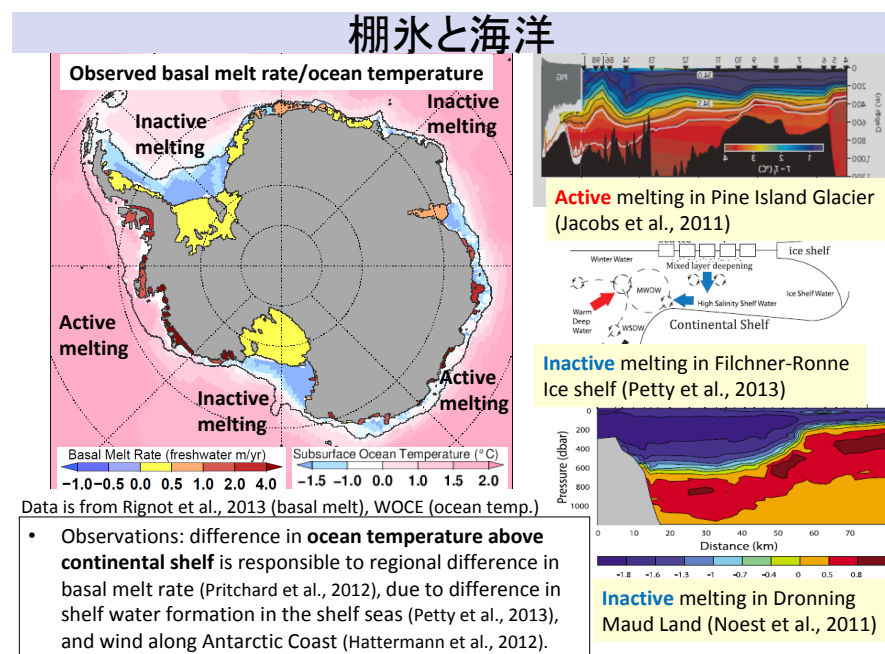


Fig. 4 | AIS stability as a function of the imposed regional annual mean temperature anomaly. **a,b**, Changes in SMB (a) and SLR contribution (b) for the AIS relative to 2000 ce as simulated under spatially uniform temperature increases that follow RCP trajectories to 2300 ce and then stabilize³⁰. Coloured lines denote different years (ce); data are averages of high and low scenarios, denoting two different grounding-line parameterizations. Grey shading shows the approximate equivalent global mean temperature anomaly for an Antarctic mean temperature anomaly of 1.5–2.0 °C, accounting for polar amplification.

Tipping points

- 南極氷床のTipping pointは2種類ある。1つは、Ocean側のtipping pointである。Ocean meltが5m/yr以上になるtipping point. これは大陸棚周辺の地形など海底地形や海洋循環に依存している。
- 2つめは、大きなocean meltに対して、棚氷／氷床システムがどのくらい解けるか、という氷床側のTipping pointである。



Tipping points

- 海洋モデル: 温度の上昇→meltの関係を地域ごとに出す。(Obase, Abe-Ouchi, Kusahara and Hasumi, 2017, Journal of Climate)
- 氷床モデル: 大きな温度変化に対して(海洋および大気)、棚氷／氷床システムがどのくらい解けるか？

